

Copyright © 1976, by the author(s).
All rights reserved.

Permission to make digital or hard copies of all or part of this work for personal or classroom use is granted without fee provided that copies are not made or distributed for profit or commercial advantage and that copies bear this notice and the full citation on the first page. To copy otherwise, to republish, to post on servers or to redistribute to lists, requires prior specific permission.

A NEW ANALYTICAL REPRESENTATION FOR SECTION-WISE
PIECEWISE-LINEAR FUNCTIONS AND ITS APPLICATIONS

by

Leon O. Chua and Sung Mo Kang

Memorandum No. ERL-M585

29 March 1976

ELECTRONICS RESEARCH LABORATORY

College of Engineering
University of California, Berkeley
94720

A NEW ANALYTICAL REPRESENTATION FOR SECTION-WISE
PIECEWISE-LINEAR FUNCTIONS AND ITS APPLICATIONS

Leon O. Chua[†] and Sung Mo Kang^{††}

ABSTRACT

This paper presents a new closed form analytical formula for representing n -dimensional surfaces and scalar functions of n variables which are piecewise-linear over each cross section obtained by freezing any combination of $n-1$ of the n coordinates. This new section-wise piecewise-linear representation can be easily programmed with efficient computer storage. It is a global representation in the sense that a single formula is used to compute for $f(x_1, x_2, \dots, x_n)$ for all values of (x_1, x_2, \dots, x_n) . Since this representation is expressed in closed analytic form, it allows standard mathematical operations and manipulations to be carried out in theoretical studies. In particular, it led to the possibility of deriving explicit closed form expressions for system parameters and design formulas. Examples are given which illustrate the potential applications of this representation in the modeling and analysis of nonlinear devices, circuits and systems.

Research supported in part by the Office of Naval Research Contract N0014-76-C-0572 and the National Science Foundation Grant ENG75-22282.

[†]L. O. Chua is with the Dept. of Electrical Engineering and Computer Sciences and the Electronics Research Laboratory, University of California, Berkeley, CA 94720.

^{††}S. M. Kang is with the Dept. of Electrical Engineering, Rutgers University, New Brunswick, N.J. 08903.

INTRODUCTION

Piecewise-linear approximation of one or more cross sections of nonlinear multi-dimensional characteristics and surfaces has been widely used in many fields of science [1-6] and Engineering [7-14]. The main motivation for its wide usage lies in the possibility for taking advantage of well-established linear techniques of analysis over each region where the characteristic is linear. Another reason for resorting to piecewise-linear approximations is that no computationally efficient techniques are currently available for approximating functions of several variables [15]. Although more efficient n-dimensional generalizations of the promising spline function approach [16] may someday be developed, its use will tend to complement rather than compete with piecewise-linear approximations.

There are three major disadvantages in current piecewise-linear approximation techniques: First, the lack of an explicit analytical representation precludes the possibility of carrying out any analytical studies involving piecewise-linear functions. This has restricted current piecewise-linear applications to either numerical calculations [17] or graphical analysis [12]. The second drawback is the need to store an immense amount of data for high-dimensional functions in order that the linear equations over each region in the n-dimensional space \mathbb{R}^n may be retrieved for computation purposes. The third drawback is the high overhead cost usually involved in programming and bookkeeping operations and manipulations involving piecewise-linear functions.

Our objective in this paper is to present an explicit analytical representation for multi-dimensional functions $f(x_1, x_2, \dots, x_n)$ which is piecewise-linear over each cross-section in \mathbb{R}^n defined by holding any n-1 coordinates fixed. We call this a section-wise piecewise-linear representation to emphasize the fact that while our representation agrees with the conventional piecewise-linear representation for functions of one variable ($n=1$), it is not a piecewise-linear representation when $n > 1$. On the contrary, our canonical representation for $n \geq 2$ is at least quadratic in the sense that it contains all product term combinations such as $x_j, x_j x_k, x_j x_k x_l, \dots, x_j x_k \dots x_n$. In fact, our representation is somewhat reminiscent of the tensor product approach usually used for approximating functions of n-variables [15]. However, our representation has the important advantage that all coefficients can be efficiently computed. Moreover, since our representation is expressed in analytic form, it is a global representation requiring simple programming efforts while allowing

efficient data storage and retrieval. But above all, our closed form representation allows standard mathematical operations and manipulations to be performed on equations involving section-wise piecewise-linear representations. In particular, explicit coefficients, parameters, and design formulas for many practical problems can now be derived in closed form.

The following material is divided into two parts. Part I presents the closed form canonical formulas for representing any section-wise piecewise-linear functions while Part II presents some properties and applications of these representations. In particular, canonical representations are given for piecewise-linear functions of a single variable with finite jump discontinuities in Section I-A, and that for functions of two variables in Section I-B. Further generalizations are given in Section I-C for multivalued functions, and in Section I-D for functions of n variables. Since all these canonical representations are based on the closed form equation given in Section I-A for piecewise-linear functions of a single variable, some properties of this fundamental representations which are particularly relevant to the modeling and analysis of nonlinear devices [18], circuits [17], and systems [19] are presented in Section II-A. Finally, three application of our "section-wise piecewise-linear" representations are given in Section II-B to illustrate their potential applications.

PART I: CANONICAL REPRESENTATIONS

A. A Canonical Piecewise-Linear Representation for Single-Valued Functions with Finite Jump Discontinuities

A typical piecewise-linear function with finite jump discontinuities is shown in Fig. 1. We will always label the segments consecutively from "0" (left-most segment) through "n" (rightmost segment) and let " m_j " denote the slope of segment j. Corresponding to the $n+1$ segments, partition the x-axis into $n+1$ intervals $I_0 \triangleq (-\infty, x_1]$, $I_1 \triangleq (x_1, x_2]$, ..., $I_{n-1} \triangleq (x_{n-1}, x_n]$, and $I_n \triangleq (x_n, \infty)$, as shown in Fig. 1(b). If we let segment k be represented by an "affine" equation

$$f(x) = \alpha_k + \beta_k x \triangleq f|_{I_k}, \quad x_k < x \leq x_{k+1} \quad (1)$$

then we can define the following associated extension operator:

$$\overrightarrow{f|_{I_k}} \triangleq \begin{cases} 0, & x \leq x_k \\ \alpha_k + \beta_k x, & x > x_k \end{cases} \quad (2)$$

Graphically, $\overrightarrow{f|_{I_k}}$ is simply a two-segment piecewise-linear function where the

left segment coincides with the x-axis over $(-\infty, x_k]$ and the right segment is obtained by extending segment k of the piecewise-linear function $f(x)$ over (x_k, ∞) . Using this notation, we can develop the following algorithm which gives the value of $f(x)$ over each interval I_k :

Piecewise-Linear Function Evaluation Algorithm

Let $f(x)$ be a piecewise-linear function with $n+1$ segments.

Step 1: Set $f^0(x) \triangleq \alpha_0 + \beta_0 x, x \in (-\infty, \infty)$ (3)

Set $f^0|_{I_0} \triangleq f^0(x), x \in I_0$ (4)

Set $k = 1$.

Step 2: Compute $\overrightarrow{\Delta f_k(x)} \triangleq \overrightarrow{f|_{I_k}} - \overrightarrow{f^{k-1}|_{I_k}}$ (5)

where $\overrightarrow{f^{k-1}|_{I_k}}$ denotes the extension operator applied to the function $f^{k-1}(\cdot)$ as defined in (2).

Step 3: Set $f^k(x) \triangleq f^{k-1}(x) + \overrightarrow{\Delta f_k(x)}, x \in (-\infty, \infty)$ (6)

Step 4: If $k < n$, set $k = k + 1$ and go to step 2.

Otherwise, stop.

After n iterations, the preceding algorithm generates $n+1$ functions $f^0(x), f^1(x), \dots, f^n(x)$ for all $x \in (-\infty, \infty)$. It is easy to see by geometrical construction that the value of $f(x)$ over any interval I_k is simply given by

$f(x) = f^k(x), x \in I_k$ (7)

Observe that (5) and (7) imply

$\overrightarrow{\Delta f_k(x)} = \begin{cases} 0, & x \leq x_k \\ \gamma_k + \delta_k(x-x_k), & x > x_k \end{cases}$ (8)

where

$\gamma_k \triangleq f(x_k^+) - f(x_k^-)$ (9)

denotes the amount of jump in $f(x)$ at $x = x_k$, and

$\delta_k \triangleq$ slope of $\overrightarrow{\Delta f_k(x)}$ for $x > x_k$ (10)

Observe from (8) that $\overrightarrow{\Delta f_k(x)}$ can be expressed in analytic form using only the

absolute-value function $|\cdot|$ and the sign function $\text{sgn}(\cdot)$; namely,¹

$$\overrightarrow{\Delta f_k(x)} = \frac{1}{2} \delta_k \left\{ |x-x_k| + (x-x_k) \right\} + \frac{1}{2} \gamma_k \left\{ 1 + \text{sgn}(x-x_k) \right\} \quad (11)$$

It follows from (6) and the observation $\overrightarrow{\Delta f_k(x)} = 0$ whenever $x \leq x_k$ that the following general expression is valid for any $x \in (-\infty, \infty)$:

$$\begin{aligned} f(x) &= f^n(x) \\ &= f^{n-1}(x) + \overrightarrow{\Delta f_n(x)} \\ &= \left[f^{n-2}(x) + \overrightarrow{\Delta f_{n-1}(x)} \right] + \overrightarrow{\Delta f_n(x)} \\ &\vdots \\ &= f^0(x) + \sum_{j=1}^n \overrightarrow{\Delta f_j(x)} \end{aligned} \quad (12)$$

Substituting (3) and (11) into (12) and combining terms, we obtain the following canonical representation:

$$f(x) = a_0 + a_1 x + \sum_{j=1}^n \left\{ b_j |x-x_j| + c_j \text{sgn}(x-x_j) \right\} \quad (13)$$

where the coefficients a_0 , a_1 , b_j , and c_j are functions of the parameters α_0 , β_0 , δ_k , and γ_k defined earlier in (3), (9), and (10). We are now ready to present the main result in this paper which provides an explicit closed form formula for determining these coefficients directly:

Main Theorem: Canonical Piecewise-Linear Representation

Any single-valued piecewise-linear function with at most n finite jump discontinuities at the n breakpoints $x_1 < x_2 < \dots < x_n$ can be represented uniquely by (13), where the coefficients are given explicitly by:²

$$a_1 = \frac{1}{2}(m_0 + m_n) \quad (14)$$

$$b_j = \frac{1}{2}(m_j - m_{j-1}), \quad j = 1, 2, \dots, n \quad (15)$$

$$c_j = \begin{cases} 0, & \text{if } f(\cdot) \text{ is continuous at the breakpoint } x = x_j \\ \frac{1}{2} [f(x_j^+) - f(x_j^-)], & \text{otherwise} \end{cases} \quad (16)$$

$$a_0 = f(0) - \sum_{j=1}^n (b_j |x_j| - c_j \text{sgn}(x_j)) \quad (17)$$

¹We define $|x| \triangleq \begin{cases} x, & x > 0 \\ -x, & x \leq 0 \end{cases}$ and $\text{sgn}(x) \triangleq \begin{cases} 1, & x > 0 \\ -1, & x \leq 0 \end{cases}$

²Recall m_j denotes the slope of segment j .

Proof: The canonical expression for $f(x)$ has already been shown to be given by (13). It suffices therefore for us to derive (14)-(17). For all $x \neq x_j$, $j = 1, 2, \dots, n$, (13) implies that

$$f'(x) = a_1 + \sum_{j=1}^n b_j \operatorname{sgn}(x-x_j) \quad (18)$$

The slope m_j of segment j of $f(x)$ can be evaluated directly from (18); namely,

$$m_0 = a_1 - \sum_{j=1}^n b_j \quad (19)$$

$$m_1 = a_1 + b_1 - \sum_{j=2}^n b_j \quad (20)$$

$$\vdots$$

$$m_k = a_1 + \sum_{j=1}^k b_j - \sum_{j=k+1}^n b_j \quad (21)$$

$$\vdots$$

$$m_n = a_1 + \sum_{j=1}^n b_j \quad (22)$$

It follows from (19) and (22) that $a_1 = \frac{1}{2}(m_0 + m_n)$, which is (14). Similarly, letting $k=j$ and $j-1$, respectively, in (21), and subtracting the resulting equations, we obtain (15). Finally, (16) follows from (9) and (11), while (17) follows from (13). ■

Example 1.

Consider the piecewise-linear function $f(x)$ in Fig. 2 with breakpoints at $x_1 = -4$, $x_2 = -2$, $x_3 = 0$, and $x_4 = 2$. The slopes are given by $m_0 = 1$, $m_1 = 1$, $m_2 = -1$, $m_3 = \frac{1}{2}$, and $m_4 = 2$. Substituting these data into (14)-(17), we obtain $a_1 = \frac{3}{2}$, $b_1 = 0$, $b_2 = -1$, $b_3 = b_4 = \frac{3}{4}$; $c_1 = \frac{1}{2}$, $c_2 = c_3 = 0$, $c_4 = 1$, and $a_0 = -1$. Substituting these coefficients into (13), we obtain

$$f(x) = -1 + \frac{3}{2}x + \frac{1}{2} \operatorname{sgn}(x+4) - |x+2| + \frac{3}{4}(|x| + |x-2|) + \operatorname{sgn}(x-2) \quad (23) \quad \blacksquare$$

B. A Canonical Piecewise-Linear Representation for a Family of Single-Valued Functions with Jump Discontinuities

The dc characteristic curves of 3-terminal devices, such as transistors, FET's, etc., are generally modeled by a set of input characteristics and a set of output characteristics, respectively [12, 17]. Each set is usually measured by a curve tracer [20] and, for large-signal applications, the characteristics can often be approximated realistically by a family of piecewise-linear curves

$$y = f(x,p) \quad (24)$$

where p denotes a parametric variable. For example, the collector characteristics of a transistor would assume the form $I_C = f(V_{CE}, I_B)$, where I_C and V_{CE} denote the collector current and the collector-to-emitter voltage, respectively. In this case, the base current I_B is the parametric variable. Our objective in this section is to show that (24) can also be represented by a canonical form similar to that of (13).

Let $\mathcal{F} = \left\{ y = f(x, p) : p = p_1, p_2, \dots, p_N \right\}$ denote a family of single-valued piecewise-linear curves having finite jump discontinuities. Without loss of generality, we can assume each piecewise-linear curve $f(x, p_i)$ has n breakpoints $x_1(p_i) < x_2(p_i) < \dots < x_n(p_i)$, and $n+1$ segments with slopes $m_0(p_i), m_1(p_i), \dots, m_n(p_i)$, respectively. Such a curve can obviously be represented by (13). Now if we let p assume the N values assigned to the given curves in \mathcal{F} , we can represent each curve in \mathcal{F} exactly by the following section-wise piecewise-linear canonical representation:

$$f(x, p) = a_0(p) + a_1(p)x + \sum_{j=1}^n \left\{ b_j(p) \cdot |x - x_j(p)| + c_j(p) \operatorname{sgn}(x - x_j(p)) \right\} \quad (25)$$

where $a_0(\cdot), a_1(\cdot), b_j(\cdot),$ and $c_j(\cdot)$ are given respectively by

$$a_1(p) = \frac{1}{2} [m_0(p) + m_n(p)] \quad (26)$$

$$b_j(p) = \frac{1}{2} [m_j(p) - m_{j-1}(p)] \quad (27)$$

$$c_j(p) = \begin{cases} 0, & \text{if } f(x, p) \text{ is continuous at the breakpoint } x = x_j(p) \\ \frac{1}{2} [f(x_j^+(p), p) - f(x_j^-(p), p)], & \text{otherwise} \end{cases} \quad (28)$$

$$a_0(p) = f(0, p) - \sum_{j=1}^n \left\{ b_j(p) \cdot |x_j(p)| - c_j(p) \operatorname{sgn}(x_j(p)) \right\} \quad (29)$$

Observe that (25) is completely specified by at most $3n+2$ functions of a single variable p ; namely, $a_0(p), a_1(p), b_j(p), c_j(p),$ and $x_j(p), j = 1, 2, \dots, n$, where n is the number of breakpoints in each curve in \mathcal{F} . Moreover, if all curves in \mathcal{F} are continuous, then $c_j(p) \equiv 0$ and only $2n+2$ functions are needed. These functions may be represented by any convenient interpolation scheme, such as Lagrange or Hermite polynomial [21], or by any convenient analytical formula such as the piecewise-linear representation given in (13). Since the interpolation formulas are chosen such that $a_1(p_i), b_j(p_i), c_j(p_i), x_j(p_i)$ and $a_0(p_i)$ are equal exactly to those computed from the given data via (26)-(29), it is clear that (25) gives an exact model of all piecewise-linear curves given in the family \mathcal{F} . For those

values of $p \neq p_i$ such that $p_{i-1} < p < p_i$, (25) would yield a piecewise-linear curve which lies between the two given curves $y = f(x, p_{i-1})$ and $y = f(x, p_i)$. In other words, (25) is a global representation which automatically interpolates among the given family of curves to generate other intermediate curves. Since the maximum number "3n+2" of "model functions" needed to specify (25) depends only on the number "n" of breakpoints per curve, and not on the number of curves given in \mathcal{F} , it is clear that not only does (25) provide us with a single global and exact analytical representation for \mathcal{F} , but it also results in a rather significant amount of data compression. Indeed, the larger the number "N" of curves given in \mathcal{F} , the more saving in computer storage space would result assuming that the 3n+2 model functions have been efficiently represented. Finally, we remark that the basic idea behind the section-wise piecewise-linear representation (25) is similar to that given in [22].

Example 2.

Consider the anode-to-cathode dc characteristic curves of a typical silicon-controlled rectifier (SCR) as shown in Fig. 3(a) and its 5-segment piecewise-linear approximation as shown in Fig. 3(b). In this case, $\mathcal{F} = \left\{ V_A = f(I_A, I_g) : I_g = 0, 5, 10, 15, 20 \right\}$, where the gate current I_g is the parametric variable. Observe that $n=4$ since each curve has 4 breakpoints, and $N=5$ since \mathcal{F} has 5 curves corresponding to 5 values of I_g . Since all curves in Fig. 3(b) are continuous, $c_j(I_g) \equiv 0$ and we can model the given family of curves exactly by

$$V_A = f(I_A, I_g) = a_0(I_g) + a_1(I_g)I_A + b_1(I_g) \cdot |I_A - I_1(I_g)| + b_2(I_g) \cdot |I_A - I_2(I_g)| + b_3(I_g) \cdot |I_A - I_3(I_g)| + b_4(I_g) \cdot |I_A - I_4(I_g)| \quad (30)$$

where $I_1(I_g)$, $I_2(I_g)$, $I_3(I_g)$, and $I_4(I_g)$ denote the 4 breakpoint locations for each value of $I_g = 0, 5, 10, 15, 20$, as shown in Figs. 3(c)-(f). Observe that for simplicity, the 4 breakpoints in Figs. 3(c)-(f) are connected by straight line segments, thereby allowing each breakpoint function $I_j(I_g)$ to be represented by (13). On many occasions of practical interest, however, the shape of these curves may match other well-known functions--such as exponentials or hyperbolic functions-- in which case, it would be advantageous to choose these functions instead. Additional data reduction is often achieved by a clever choice of such functions. For example, an exponential function would require only 3 parameters for complete characterization, whereas a 4-segment continuous piecewise-linear representation via (13) would require 10 parameters.

Since $n=4$ and since $c_j(I_g) \equiv 0$, (30) requires only $2n+2 = 10$ model functions; namely, $a_0(I_g)$, $a_1(I_g)$, $b_j(I_g)$ and $I_j(I_g)$, $j = 1,2,3,4$. The functions $a_0(\cdot)$, $a_1(\cdot)$, and $b_j(\cdot)$ are determined from (26), (27), and (29) and are shown in Figs. 3(g)-(1). Again, for complete generality, we represent these functions by piecewise-linear curves so that they can in turn be represented by (13). A more careful analysis with specific devices would often suggest the use of other well-known functions requiring fewer numbers of parameters. Observe also that further simplification may be achieved by approximating each curve in Fig. 3(a) by 3 segments rather than 4. In this case, $n=2$ and only 6 model functions would be needed to completely specify the model.

A comparison between the canonical representation for functions of a single variable given by (13) with that of the canonical representation for functions of two variables given by (25) reveals a rather significant difference; namely, whereas (13) represents truly a one-dimensional piecewise-linear function, (25) does not represent a two-dimensional piecewise-linear function. In fact, if the model functions $a_0(\cdot)$, $a_1(\cdot)$, $b_j(\cdot)$, $c_j(\cdot)$, and $x_j(\cdot)$ are represented by polynomials, the (25) represents a piecewise-linear curve only for fixed value of the parameter p . In other words, (25) can be said to be a sectionwise piecewise-linear representation. The overall function is, however, nonlinear since (25), when expanded, contains such quadratic terms as xp .

C. A Canonical Piecewise-Linear Representation for Multivalued Relations

The representations given in the preceding section are valid only for single-valued functions. Our objective in this section is to present yet another canonical representation for an important class of multivalued piecewise-linear curves; namely, the class of parametrizable, or unicursal curves. It is shown in [12] that any unicursal curve $g(x,y) = 0$ can be represented by two single-valued functions of a common parametric variable ρ ; namely, $x = x(\rho)$ and $y = y(\rho)$. For example, an ideal diode characterized by the multivalued curve shown in Fig. 4(a) can be represented analytically by

$$i = \frac{1}{2} (|\rho| + \rho) \quad (31a)$$

$$v = \frac{1}{2} (|\rho| - \rho) \quad (31b)$$

Equation (31) represents a simple multivalued relation and could have been derived by inspection. For more complicated curves, such as the one shown in Fig. 4(b), an explicit canonical representation would be extremely useful. To

derive this representation, choose any convenient but arbitrary breakpoint, say (x_q, y_q) and label it as the parametric origin Q. Corresponding to any point P on the curve, assign a value ρ whose magnitude is equal to the total length of the curve measured from the origin Q to the point P. Since the curve is unicursal by assumption, we can assign an arbitrary orientation (denoted by arrowheads in Fig. 4(b)) to the curve and define $\rho > 0$ at P whenever point P is traced from Q in the same direction as the assigned orientation. Otherwise, define $\rho < 0$ at P.

To derive an explicit representation, it is convenient to choose an arbitrary point (x_0, y_0) on the leftmost segment, and another point (x_{n+1}, y_{n+1}) on the rightmost segment. If we let l_k denote the length of the line segment between the two breakpoints (x_k, y_k) and (x_{k+1}, y_{k+1}) , then

$$l_k = \left[(x_{k+1} - x_k)^2 + (y_{k+1} - y_k)^2 \right]^{\frac{1}{2}}, \quad k = 0, 1, 2, \dots, n \quad (32)$$

and the distance ρ_k , i.e., total length, from the origin Q at breakpoint (x_q, y_q) to any other breakpoint (x_k, y_k) is given by

$$l_k = \begin{cases} \sum_{j=q}^{k-1} l_j, & \text{if } k > q \\ -\sum_{j=k}^{q-1} l_j, & \text{if } k < q \end{cases} \quad (33)$$

where $k = 1, 2, \dots, n$. Equation (33) provides us with the exact coordinates for the breakpoints of the parametric representations $x = x(\rho)$ and $y = y(\rho)$ of $g(x, y) = 0$. Hence, if we define the slopes m_k^x and m_k^y for segment k of $x(\rho)$ and $y(\rho)$ respectively by

$$m_k^x \triangleq (x_{k+1} - x_k) / l_k, \quad k = 0, 1, 2, \dots, n \quad (34a)$$

$$m_k^y \triangleq (y_{k+1} - y_k) / l_k, \quad k = 0, 1, 2, \dots, n \quad (34b)$$

then the canonical representations $x = x(\rho)$ and $y = y(\rho)$ for any unicursal piecewise-linear curve are given as follows:³

$$x(\rho) = a_0^x + a_1^x \rho + \sum_{j=1}^n b_j^x |\rho - \rho_j| \quad (35a)$$

³It is easy to see that $x = x(\rho)$ and $y = y(\rho)$ are continuous functions even though the given multivalued curve may contain vertical segments. This means that $c_j = 0$ in (13).

where

$$a_1^x = \frac{1}{2}(m_0^x + m_n^x) \quad (36a)$$

$$b_j^x = \frac{1}{2}(m_j^x - m_{j-1}^x), \quad j = 1, 2, \dots, n \quad (37a)$$

$$a_0^x = x_q - \sum_{j=1}^n b_j^x |\rho_j| \quad (38b)$$

and

$$y(\rho) = a_0^y + a_1^y \rho + \sum_{j=1}^n b_j^y |\rho - \rho_j| \quad (35b)$$

where

$$a_1^y = \frac{1}{2}(m_0^y + m_n^y) \quad (36b)$$

$$b_j^y = \frac{1}{2}(m_j^y - m_{j-1}^y), \quad j = 1, 2, \dots, n \quad (37b)$$

$$a_0^y = y_q = \sum_{j=1}^n b_j^y |\rho_j| \quad (38b)$$

Example 3

Consider the unicursal $v-i$ curve shown in Fig. 5(a). This curve has 11 breakpoints. For the two additional points on the leftmost and rightmost segments needed to compute the slope of these two segments, let us choose the points located at $(-4, 3)$ and $(5, 3)$ (labelled as point 0 and 12 on the curve). If we choose the breakpoint 5 at $(-2, -1)$ as the origin Q , and apply the canonical representations given by (35-38), we would obtain

$$v(\rho) = a_0^v + a_1^v \rho + \sum_{j=1}^{11} b_j^v |\rho - \rho_j| \quad (39a)$$

where

$$a_0^v = -11.73, \quad a_1^v = 0.38; \quad b_1^v = 0.51, \quad b_2^v = 0.71, \quad b_3^v = -0.19, \quad b_4^v = -0.51, \\ b_5^v = 0.71, \quad b_6^v = -0.08, \quad b_7^v = -0.78, \quad b_8^v = 0.73, \quad b_9^v = 0.22, \quad b_{10}^v = 0.45, \quad \text{and} \\ b_{11}^v = 0.22.$$

$$\text{and } i(\rho) = a_0^i + a_1^i \rho + \sum_{j=1}^{11} b_j^i |\rho - \rho_j| \quad (39b)$$

where

$$a_0^i = -13.59, \quad a_1^i = -0.03, \quad b_1^i = 0.83, \quad b_2^i = 0, \quad b_3^i = -0.83, \quad b_4^i = 0.83, \quad b_5^i = 0, \\ b_6^i = -0.77, \quad b_7^i = 0.42, \quad b_8^i = -0.45, \quad b_9^i = 0.67, \quad b_{10}^i = 0.27, \quad \text{and } b_{11}^i = -0.05.$$

The breakpoints for both $v(\rho)$ and $i(\rho)$ are of course identical and are located as follow:

$$\rho_1 = -10.23, \rho_2 = -7.41, \rho_3 = -4.58, \rho_4 = -1.41, \rho_5 = 0, \rho_6 = 4.24, \rho_7 = 7.85, \\ \rho_8 = 9.85, \rho_9 = 12.08, \rho_{10} = 14.3, \text{ and } \rho_{11} = 17.32.$$

The curves corresponding to (39a) and (39b) are plotted as shown in Fig. 5(b) and (c), respectively. A comparison of these two curves with its associated multi-valued curve shown in Fig. 5(a) would verify the validity of the canonical representations (35a) and (35b).

D. A Canonical Sectionwise-Piecewise-Linear Representation for Continuous Functions of Several Variables

Our objective in this section is to generalize the basic approach presented in Section II-B and develop a canonical representation for continuous functions $y = f(x_1, x_2, \dots, x_n)$ of n variables. We assume a priori that a sufficient number of data points has been taken such that the function can be realistically approximated by a piecewise-linear function of a single variable along every cross-section obtained by freezing any combination of $(n-1)$ of the n coordinates.

Consider first the case $n=3$ and suppose that the values of $f(x_1, x_2, x_3)$ are given at a set of N^3 data points (x_{1i}, x_{2j}, x_{3k}) , $i, j, k = 1, 2, \dots, N$. By assumption, the function $f(x_{1i}, x_{2j}, x_{3k})$ with the second and third coordinates fixed at $x_2 = x_{2j}$ and $x_3 = x_{3k}$ is a piecewise-linear continuous function of a single variable x_1 and can therefore be represented by (13); namely,⁴

$$f(x_1, x_{2j}, x_{3k}) = a_0(x_{2j}, x_{3k}) + a_1(x_{2j}, x_{3k}) + \sum_{i=1}^{N-2} b_i(x_{2j}, x_{3k}) |x_1 - x_{1i}| \quad (40)$$

where the coefficients a_0 , a_1 and b_i are determined via (17), (14) and (15), respectively. Notice that these coefficients will change for a different choice of (x_{2j}, x_{3k}) and hence can be considered as functions of the two variables x_2 and x_3 whose values at any data point (x_{2j}, x_{3k}) can be computed from (17), (14) and (15). Since $a_0(x_2, x_3)$, $a_1(x_2, x_3)$, and $b_i(x_2, x_3)$ are now functions of two instead of the original three variables, they can be represented in turn by the canonical representation (25). It follows from the preceding algorithm that

⁴The upper index of summation in (40) is $N-2$, rather than N because the leftmost and the rightmost data points are needed to compute for the slope of the two end segments, and hence only $N-2$ data points are available as breakpoints. We are implicitly assuming as always that the two leftmost (resp., rightmost) data points lie on a straight line extending to $-\infty$ (resp., $+\infty$).

any continuous function $f(x_1, x_2, x_3)$ of three variables having a piecewise-linear cross section can be represented by the following canonical form

$$f(x_1, x_2, x_3) = a_0(x_2, x_3) + a_1(x_2, x_3)x_1 + \sum_{i=1}^{N-2} b_j(x_2, x_3) |x_1 - x_{1i}| \quad (41)$$

where

$$a_0(x_2, x_3) = a_0^{a_0}(x_3) + a_1^{a_0}(x_3)x_2 + \sum_{i=1}^{N-2} b_j^{a_0}(x_3) |x_2 - x_{2i}| \quad (42)$$

$$a_1(x_2, x_3) = a_0^{a_1}(x_3) + a_1^{a_1}(x_3)x_2 + \sum_{i=1}^{N-2} b_j^{a_1}(x_3) |x_2 - x_{2i}| \quad (43)$$

$$b_j(x_2, x_3) = a_0^{b_j}(x_3) + a_1^{b_j}(x_3)x_2 + \sum_{i=1}^{N-2} b_i^{b_j}(x_3) |x_2 - x_{2i}| \quad (44)$$

where the double superscripts attached to the coefficients $a_0(x_3)$, $a_1(x_3)$, and $b_j(x_3)$ are used to identify the associated model function. Observe that the model functions in (42)-(44) are now all functions of a single variable x_3 , and hence can in turn be represented by (13).

The generalization of the preceding algorithm to continuous functions of any number "n" of variables is now obvious. We first freeze all (n-1) coordinates x_2, x_3, \dots, x_n and write

$$\boxed{f(x_1, x_2, x_3, \dots, x_n) = a_0(x_2, x_3, \dots, x_n) + a_1(x_2, x_3, \dots, x_n)x_1 + \sum_{j=1}^{N-2} b_j(x_2, x_3, \dots, x_n) |x_1 - x_{1j}|} \quad (45)$$

where $a_0(x_2, x_3, \dots, x_n)$, $a_1(x_2, x_3, \dots, x_n)$, and $b_j(x_2, x_3, \dots, x_n)$ are functions of n-1 variables, which is one less than the original number of variables. The same algorithm can be applied repeatedly to these model functions, where the number of variables is reduced by one after each iteration. The algorithm must clearly terminate when all model functions have been reduced to functions of a single variable, which in turn are represented by (13). The following example illustrates the steps involved in this algorithm.

Example 4.

Suppose the function to be represented is given by ⁵

⁵We specify the function $f(x_1, x_2, x_3)$ here by an equation in order to check the validity of our canonical representation for this example. In practice, this function is usually available only as a table of values of $f(\cdot)$ measured at a set of data points.

$$f(x_1, x_2, x_3) = (1+x_1+|x_1-1|)(1+x_2+|x_2-1|)(1+x_3+|x_3-1|) \quad (46)$$

For simplicity, let us choose the set S of data points to be uniformly distributed on the cubical lattice as shown in Fig. 6(a); namely,

$$S = \left\{ (x_{1i}, x_{2j}, x_{3k}) : i, j, k = 1, 2, 3 \right\}, \quad x_{1i}, x_{2j}, x_{3k} \in \{0, 1, 2\} \quad (47)$$

Here $N=3$ and we have a total of $N^3 = 27$ data points where the value of f is assumed to be specified. For this example, the value of f at each of these 27 data points is simply obtained by direct substitution of (x_{1i}, x_{2j}, x_{3k}) into (46). In practice, these values must either be measured from the surface representing $f(x_1, x_2, x_3)$, or must be computed in accordance with some algorithm germane to the problem on hand. Since $N=3$ and $N-2=1$ in this case, the canonical representation (41) assumes the form

$$f(x_1, x_2, x_3) = a_0(x_2, x_3) + a_1(x_2, x_3)x_1 + b_1(x_2, x_3)|x_1-1| \quad (48)$$

Observe that for each cross section $x_2 = x_{2j}$ and $x_3 = x_{3k}$, $f(x_1, x_{2j}, x_{3k})$ is a continuous piecewise-linear function representing a 2-segment curve sharing a common breakpoint. Our next task is to determine the coefficients $a_0(x_{2j}, x_{3k})$, $a_1(x_{2j}, x_{3k})$ and $b_1(x_{2j}, x_{3k})$ for each combination of the indices $j, k = 1, 2, 3$. Since the procedures for determining these coefficients are identical in each case, we will show the detailed calculation for only one case; namely, the cross section corresponding to $j=1, k=1$:

Cross section 1: $x_2 = x_{21} = 0, x_3 = x_{31} = 0$

It follows from (48) that

$$f(x_1, 0, 0) = f(x_1, x_{21}, x_{31}) = a_0(0, 0) + a_1(0, 0)x_1 + b_1(0, 0)|x_1-1|$$

To determine the coefficients $a_0(0, 0)$, $a_1(0, 0)$, and $b_1(0, 0)$, we need the values of $f(x_1, x_2, x_3)$ at the three points $(x_{11}, 0, 0)$, $(x_{12}, 0, 0)$, and $(x_{13}, 0, 0)$; namely, $f(x_{11}, 0, 0) = f(0, 0, 0) = 8$, $f(x_{12}, 0, 0) = f(1, 0, 0) = 8$, and $f(x_{13}, 0, 0) = f(2, 0, 0) = 16$ (these values are computed directly from (46) in this example). Since $f(x_1, 0, 0)$ is piecewise-linear, by assumption, these three values of $f(\cdot, 0, 0)$ determined uniquely a piecewise-linear curve as shown in Fig. 6(b). Observe that the first two data points $(0, 8)$ and $(1, 8)$ are used to obtain the slope $m_0=0$ for segment 0, whereas the last two data points $(1, 8)$ and $(2, 16)$ are used to obtain the slope $m_1=8$ for segment 1. With $m_0=0$, $m_1=8$, and the breakpoint

location $x_1=1$ now known, $a_1(0,0)$, $b_1(0,0)$, and $a_0(0,0)$ can be computed from (14), (15), and (17); namely, $a_1(0,0) = \frac{1}{2}(0+8) = 4$, $b_1(0,0) = \frac{1}{2}(8-0) = 4$, and $a_0(0,0) = f(0,0,0) - (4)(1) = 4$.

Repeating the above procedure to each of the remaining cross sections, the corresponding coefficients can be computed and the result is summarized in Table 1:

Table 1. Calculated Coefficients for Different Cross Sections

Cross Section $x_2 = x_{2j}, x_3 = x_{3k}$		$a_0(x_2, x_3)$	$a_1(x_2, x_3)$	$b_1(x_2, x_3)$
1	$x_2 = 0, x_3 = 0$	$a_0(0,0) = 4$	$a_1(0,0) = 4$	$b_1(0,0) = 4$
2	$x_2 = 0, x_3 = 1$	$a_0(0,1) = 4$	$a_1(0,1) = 4$	$b_1(0,1) = 4$
3	$x_2 = 0, x_3 = 2$	$a_0(0,2) = 8$	$a_1(0,2) = 8$	$b_1(0,2) = 8$
4	$x_2 = 1, x_3 = 0$	$a_0(1,0) = 4$	$a_1(1,0) = 4$	$b_1(1,0) = 4$
5	$x_2 = 1, x_3 = 1$	$a_0(1,1) = 4$	$a_1(1,1) = 4$	$b_1(1,1) = 4$
6	$x_2 = 1, x_3 = 2$	$a_0(1,2) = 8$	$a_1(1,2) = 8$	$b_1(1,2) = 8$
7	$x_2 = 2, x_3 = 0$	$a_0(2,0) = 8$	$a_1(2,0) = 8$	$b_1(2,0) = 8$
8	$x_2 = 2, x_3 = 1$	$a_0(2,1) = 8$	$a_1(2,1) = 8$	$b_1(2,1) = 8$
9	$x_2 = 2, x_3 = 2$	$a_0(2,2) = 16$	$a_1(2,2) = 16$	$b_1(2,2) = 16$

Our final task is to model $a_0(x_2, x_3)$, $a_1(x_2, x_3)$, and $b_1(x_2, x_3)$ via (25) which now assume the form:

$$a_0(x_2, x_3) = a_0^{a_0}(x_3) + a_1^{a_0}(x_3)x_2 + b_1^{a_0}(x_3)|x_2-1| \quad (49)$$

$$a_1(x_2, x_3) = a_0^{a_1}(x_3) + a_1^{a_1}(x_3)x_2 + b_1^{a_1}(x_3)|x_2-1| \quad (50)$$

$$b_1(x_2, x_3) = a_0^{b_1}(x_3) + a_1^{b_1}(x_3)x_2 + b_1^{b_1}(x_3)|x_2-1| \quad (51)$$

An inspection of Table 1 shows that for this example, the values assumed by these three functions are identical at the specified data points and hence we only have to determine one of them, say $a_0(x_2, x_3)$. The values assumed by this function are

plotted in Fig. 6(c). By assumption, $a_0(\cdot, x_{3k})$ is a piecewise-linear function on each cross section $x_3 = x_{3k}$, $k = 1, 2, 3$. This assumption allows us to pass straight-line segments through the data points as shown in Fig. 6(c), for the three cross sections $x_3 = x_{31} = 0$, $x_3 = x_{32} = 1$, and $x_3 = x_{33} = 2$. Hence, the data needed to determine $a_0^{a_0}(x_{3k})$, $a_1^{a_1}(x_{3k})$, and $b_1^{a_0}(x_{3k})$ for each value of x_{3k} are either available or can be calculated from the data given in Table 1. Applying the canonical representation (13) once more to each of these cross sections, we obtain

$$a_0^{a_0}(x_3) = 1 + x_3 + |x_3 - 1| \quad (52)$$

$$a_1^{a_0}(x_3) = 1 + x_3 + |x_3 - 1| \quad (53)$$

$$b_1^{a_0}(x_3) = 1 + x_3 + |x_3 - 1| \quad (54)$$

Substituting (52)-(54) into (50), we obtain

$$a_0(x_2, x_3) = 1 + x_3 + |x_3 - 1| + (1 + x_3 + |x_3 - 1|)x_2 + (1 + x_3 + |x_3 - 1|)|x_2 - 1| \quad (55)$$

Simplifying (55) and making use of our earlier observation that $a_0(\cdot)$, $a_1(\cdot)$, and $b_1(\cdot)$ are identical for this example, we obtain

$$a_0(x_2, x_3) = a_1(x_2, x_3) = b_1(x_2, x_3) = (1 + x_3 + |x_3 - 1|)(1 + x_2 + |x_2 - 1|) \quad (56)$$

Substituting (56) into (48), we obtain

$$f(x_1, x_2, x_3) = a_0(x_2, x_3)(1 + x_1 + |x_1 - 1|) = (1 + x_3 + |x_3 - 1|)(1 + x_2 + |x_2 - 1|)(1 + x_1 + |x_1 - 1|) \quad (57)$$

Observe that (57) is identical to the original function given in (46), thereby verifying the validity of our algorithm. If we expand (57), we see that $f(x_1, x_2, x_3)$ contains in addition to linear and product terms involving the absolute-value functions $|x_1 - 1|$, $|x_2 - 1|$, and $|x_3 - 1|$, also such quadratic terms as x_1x_2 , x_1x_3 , x_2x_3 , and $x_1x_2x_3$. Hence $f(x_1, x_2, x_3)$ is definitely not a piecewise-linear function of 3 variables, but rather a nonlinear function involving all possible products of the terms 1 , x_1, x_2, x_3 , $|x - x_1|$, $|x - x_2|$, and $|x - x_3|$. This observation is very significant because it shows that our canonical representation (45) for functions of n variables is much more general than conventional piecewise-linear functions and in fact resembles the widely used

multivariate approximation techniques involving tensor product terms [15]. However, our representation appears to be computationally much more efficient.

II. PROPERTIES AND APPLICATIONS

A. Properties and Manipulations of Piecewise-Linear Functions

The canonical piecewise-linear representation (13) has been shown in Part I to be the fundamental building block from which all section-wise piecewise-linear representations for functions of several variables are based. It is desirable therefore that we uncover as many properties as possible with respect to the constraints on the coefficients a_0 , a_1 , b_j , and c_j . To simplify our notations and derivations, unless otherwise stated, we will assume the function is continuous so that $c_j=0$ and (13) reduces to the form:

$$f(x) = a_0 + a_1 x + \sum_{j=1}^n b_j |x - x_j| \quad (58)$$

Property 1. If the breakpoints of $f(x)$ are such that $0 < x_1 < x_2 \dots < x_n$, then

$$a_0 = \frac{1}{2}[f(0) + f(x_n) - m_n x_n] \quad (59)$$

Proof. Substituting $x=0$ in (58) and solving for a_0 , we obtain

$$\begin{aligned} a_0 &= f(0) - \sum_{j=1}^n b_j x_j \\ &= f(0) - \frac{1}{2}(m_1 - m_0)x_1 - \frac{1}{2}(m_2 - m_1)x_2 - \frac{1}{2}(m_3 - m_2)x_3 - \dots - \frac{1}{2}(m_n - m_{n-1})x_n \\ &= \frac{1}{2} f(0) + \frac{1}{2}[f(0) + m_0 x_1 + m_1(x_2 - x_1) + \dots + m_{n-1}(x_n - x_{n-1})] - \frac{1}{2} m_n x_n \\ &= \frac{1}{2}[f(0) + f(x_n) - m_n x_n] \quad \blacksquare \end{aligned}$$

Property 2. A continuous piecewise-linear function $f(x)$ is monotone-increasing (resp., strictly monotone-increasing) if, and only if,

$$a_1 + \sum_{j=1}^k b_j - \sum_{j=k+1}^n b_j \geq 0 \text{ (resp., } > 0 \text{) for all } k = 0, 1, 2, \dots, n \quad (60)$$

Proof. $f(x)$ is monotone-increasing (resp., strictly monotone-increasing) if, and only if, for all $x \neq x_k$, $k = 0, 1, 2, \dots, n$, $f'(x) \geq 0$ (resp., > 0). Differentiating (58), we obtain (60). \blacksquare

It can be easily shown that (60) represents a system of $(n+1)$ independent linear inequalities. These inequalities define a convex polyhedron (polytope) $\Omega \subset \mathbb{R}^{n+1}$ where the coefficients $a_1, b_1, b_2, \dots, b_n$ must lie. Hence any piecewise-

linear function with at least one coefficient lying outside of Ω cannot be monotone increasing. If $f(\cdot)$ represents a v-i curve, then (60) becomes the criterion for local passivity.

Property 3. If a continuous piecewise-linear function has monotone-increasing slopes (resp., monotone-decreasing slopes) in the sense that $0 \leq m_0 < m_1 < \dots < m_n$ (resp., $m_0 > m_1 > \dots > m_n \geq 0$), then

- (1) $a_1 > 0$
- (2) $b_j > 0$ (resp., $b_j < 0$) for all $j = 1, 2, \dots, n$.
- (3) if $f(0) = 0$, then $a_0 \leq 0$ (resp., $a_0 \geq 0$)

Proof. (1) and (2) follow immediately from (60), while (3) follows from (58). ■

One important reason for seeking an explicit analytical representation of functions is to allow the possibility of carrying out mathematical operations and equation manipulations on the functions for analytical studies. The next two properties provide explicit formulas for performing two common mathematical operations; namely, finding the inverse $f^{-1}(\cdot)$ of $f(x)$ and finding composition $f \circ g$ between two functions $f(x)$ and $g(y)$.

Property 4. Let

$$y = f(x) = a_0 + a_1 x + \sum_{j=1}^n b_j |x - x_j|$$

be a continuous and strictly-increasing piecewise-linear function and let its inverse be given by

$$x = f^{-1}(y) = \hat{a}_0 + \hat{a}_1 y + \sum_{j=1}^n \hat{b}_j |y - y_j| \quad (61)$$

then the coefficients in (61) can be computed as follow:

$$\hat{a}_1 = a_1 / \left[a_1^2 - \left(\sum_{j=1}^n b_j \right)^2 \right] \quad (62)$$

$$\hat{b}_k = -b_k / \left[\left(a_1 + \sum_{j=1}^{k-1} b_j - \sum_{j=k+1}^n b_j \right)^2 - b_k^2 \right], \quad k = 1, 2, \dots, n \quad (63)$$

$$\hat{a}_0 = f^{-1}(0) - \sum_{j=1}^n \hat{b}_j |f(x_j)| \quad (64)$$

Proof. See Appendix A.

Remark. Property 4 can be generalized to allow finite jump discontinuities in $f(x)$. In this case, as is commonly done in electronic circuit literature, the two points at each jump discontinuity are connected by a vertical segment and

$f(x)$ becomes a multivalued function. The inverse $f^{-1}(x)$, however, is a well-defined single-valued function because the inverse of a vertical segment becomes a horizontal segment. To be more specific, suppose $f(x)$ is continuous except at breakpoint x_k , where $y_k^- = f(x_k^-)$ and $y_k^+ = f(x_k^+)$. Then

$$y = f(x) = a_0 + a_1 x + \sum_{\substack{j=1 \\ j \neq k}}^n b_j |x-x_j| + c_k \operatorname{sgn}(x-x_k) \quad (65)$$

and the inverse function is given by

$$x = f^{-1}(y) = \tilde{a}_0 + \tilde{a}_1 y + \sum_{\substack{j=1 \\ j \neq k}}^n \tilde{b}_j |y-y_j| + \tilde{b}_k^- |y-y_k^-| + \tilde{b}_k^+ |y-y_k^+| \quad (66)$$

It can be shown that the coefficients \tilde{a}_1 and \tilde{b}_j , $j \neq k$ in (66) can be computed from the same formulas given in (62) and (63), and that

$$\tilde{b}_k^- = -\frac{1}{2} \left[a_1 + \sum_{j=1}^{k-1} b_j - \sum_{j=k}^n b_j \right] \quad (67)$$

$$\tilde{b}_k^+ = \frac{1}{2} \left[a_1 + \sum_{j=1}^k b_j - \sum_{j=k+1}^n b_j \right] \quad (68)$$

$$\tilde{a}_0 = f^{-1}(0) - \left\{ \sum_{\substack{j=1 \\ j \neq k}}^n \tilde{b}_j |y_j| + \tilde{b}_k^- |y_k^-| + \tilde{b}_k^+ |y_k^+| \right\} \quad (69)$$

Property 5.

Let $y = f(x)$ be any piecewise-linear curve and let $x = g(z)$ be any strictly-monotone increasing piecewise-linear curve, then their composition $y \stackrel{\Delta}{=} f \circ g(z) = f(g(z)) = h(z)$ is also a piecewise-linear curve and the coefficients characterizing $h(z)$ can be computed explicitly from those characterizing $f(x)$ and $g(z)$.

In particular, if

$$y = f(x) = a_0^f + a_1^f x + \sum_{j=1}^{n_f} \left\{ b_j^f |x-x_j| + c_j^f \operatorname{sgn}(x-x_j) \right\} \quad (70)$$

$$x = g(z) = a_0^g + a_1^g z + \sum_{j=1}^{n_g} \left\{ b_j^g |z-z_j| + c_j^g \operatorname{sgn}(z-z_j) \right\} \quad (71)$$

then the composition function $f \circ g(\cdot)$ is given explicitly by:

$$y = h(z) = a_0^f + a_1^f a_0^g + \sum_{i=1}^{n_f} b_i^f \left[\sum_{j=1}^{n_g} (c_j^g - b_j^g z_j) \right] + \left[a_1^f a_1^g + \sum_{i=1}^{n_f} b_i^f \left(\sum_{j=1}^{n_g} b_j^g \right) \right] z \\ + \sum_{j=1}^{n_g} b_j^g \left(a_1^f + \sum_{i=1}^{n_f} b_i^f \operatorname{sgn}(z_j - z_i^*) \right) |z-z_j|$$

$$\begin{aligned}
& + \sum_{i=1}^{n_f} b_i^f \left(a_1^g - \sum_{j=1}^{n_g} b_j^g \operatorname{sgn}(z_j - z_i^*) \right) |z - z_i^*| \\
& + \sum_{j=1}^{n_g} c_j^g \left(a_1^f + \sum_{i=1}^{n_f} b_i^f \operatorname{sgn}(z_j - z_i^*) \right) \operatorname{sgn}(z - z_j) \\
& + \sum_{i=1}^{n_f} \left\{ b_i^f \left[a_0^g - x_i + a_1^g z_i^* + \sum_{j=1}^{n_g} \left(b_j^g |z_j - z_i^*| - c_j^g \operatorname{sgn}(z_j - z_i^*) \right) \right] \right. \\
& \quad \left. + c_i^f \right\} \operatorname{sgn}(z - z_i^*) \quad (72)
\end{aligned}$$

where z_i^* is the unique solution of $g(z) - x_i = 0$, $i = 1, 2, \dots, n_f$.

Proof. See Appendix B.

The preceding properties are particularly useful in deriving algebraically both the DP (driving-point) and TC (transfer characteristics) plots of resistive nonlinear networks. Indeed, much of the graphical procedures used for deriving DP and TC plots in [12] can now be replaced by algebraic manipulations, as the next example demonstrates.

Example 5.

Consider the nonlinear voltage divider circuit shown in Fig. 7(a) where the nonlinear resistors R_1 and R_2 are characterized by the piecewise-linear curves shown in Figs. 7(c) and (d), respectively. The problem is to derive the v_0 -vs.- v_1 TC plot.

Applying KVL and KCL, we obtain

$$v_1 = v_1 + v_0 = f(i_1) + v_0 \quad (73)$$

$$i_1 = i_2 = g(v_0) \quad (74)$$

Substituting (74) into (73), we obtain

$$v_1 = f \circ g(v_0) + v_0 \stackrel{\Delta}{=} F(v_0) \quad (75)$$

Now applying (13) to the v - i curves shown in Figs. 7(c) and (d), we obtain

$$v_1 = f(i_1) = 2i_1 - \frac{1}{2}|i_1+1| + \frac{1}{2} \operatorname{sgn}(i_1-1) + \frac{1}{2}|i_1-2| \quad (76a)$$

$$i_2 = g(v_2) = -2 + \frac{3}{2}v_2 - \frac{1}{4}|v_2+2| + \operatorname{sgn}(v_2+2) + \frac{3}{4}(|v_2| - |v_2-1| + |v_2-3|) \quad (76b)$$

Since $g(\cdot)$ is strictly monotone-increasing, the composition $f \circ g(v_0)$ is well defined. Hence substituting the corresponding coefficients defining $f(i_1)$ and $g(v_2)$ from (76a) and (76b) into (72) and simplifying the resulting expression, we obtain

$$v_i \triangleq F(v_0) = -4 + 4v_0 - \frac{3}{4}|v_0+2| + 2 \operatorname{sgn}(v_0+2) + \frac{3}{4}|v_0| + \frac{1}{2} \operatorname{sgn}(v_0 - \frac{1}{2}) - \frac{1}{2}|v_0-1| + \frac{3}{2}|v_0-3| \quad (77)$$

Since the coefficients in (77) satisfy (60) with the strict inequality sign, it follows from Property 2 that the function $F(\cdot)$ is strictly monotone-increasing and therefore has a well-defined inverse $v_0 = F^{-1}(v_i)$, which is precisely the TC plot being sought. Hence, it remains to apply Property 4 to compute $F^{-1}(\cdot)$. Observe that since $F(\cdot)$ in (77) contains a discontinuity at $v_0 = \frac{1}{2}$, we must make use of (66) rather than (64) in computing for $F^{-1}(\cdot)$. After some routine calculation and simplification, we obtain:

$$v_0 = F^{-1}(v_i) = \frac{13}{15} + \frac{4}{15} v_i - \frac{1}{6}|v_i+7| + \frac{1}{3}|v_i+3| - \frac{1}{6}|v_i| - \frac{1}{6}|v_i - \frac{3}{2}| + \frac{1}{6}|v_i - \frac{5}{2}| + \frac{1}{12}|v_i-4| - \frac{3}{20}|v_i-8| \triangleq T(v_0) \quad (78)$$

This TC plot is plotted as shown in Fig. 7(b) and can be easily verified by the graphical technique described in [12] to be the correct solution.

B. Some Applications of Canonical Piecewise-Linear Representations

In addition to the many obvious applications to approximation and computation in device, circuit, and system modeling, the canonical piecewise-linear representation is also useful in carrying out any mathematical analysis of a circuit or system where the final results in explicit analytical form are desired. Due to space limitation, only three such applications will be presented.

Application 1. Deriving Describing Functions in Explicit Form

The describing function technique has been widely used for analyzing non-linear circuits and systems subject to an input of the form $x(t) = A_0 + A_1 \cos \omega t$. The system normally has a memoryless nonlinearity $y = f(x)$ as well as some component--such as a low-pass filter--which reduces the harmonic components of $y(t)$ to negligible values. Under this assumption, we can write

$$y(t) = D_0 + D_1 \cos \omega t \quad (79)$$

where the Fourier coefficients

$$D_0(A_0, A_1) = \frac{1}{2\pi} \int_0^{2\pi} f(A_0 + A_1 \cos \phi) d\phi \quad (80)$$

and

$$D_1(A_0, A_1) = \frac{1}{\pi A_1} \int_0^{2\pi} f(A_0 + A_1 \cos \phi) \cos \phi d\phi \quad (81)$$

are called the describing functions because they depend on both A_0 and A_1 . Now if $f(x)$ is piecewise-linear, i.e.,

$$f(x) = a_0 + a_1 x + \sum_{j=1}^n (b_j |x - x_j| + c_j \operatorname{sgn}(x - x_j)) \quad (82)$$

then the following explicit formulas for $D_0(\cdot)$ and $D_1(\cdot)$ can be derived⁶ (see Appendix C):

$$D_0(A_0, A_1) = a_0 + a_1 A_0 + \frac{2}{\pi} \sum_{j=1}^n \left\{ (b_j (A_0 - x_j) + c_j) \left(\cos^{-1} \left(\frac{A_0 - x_j}{A_1} \right) - \frac{\pi}{2} \right) + b_j \sqrt{A_1^2 - (x_j - x_0)^2} \right\} \quad (83)$$

$$D_1(A_0, A_1) = a_1 + \sum_{j=1}^n \left\{ b_j + \frac{4}{\pi A_1} (b_j (A_0 - x_j) + c_j) \sqrt{1 - \left(\frac{A_0 - x_j}{A_1} \right)^2} + \frac{2b_j}{\pi} \left(\cos^{-1} \left(\frac{x_j - A_0}{A_1} \right) - \pi \right) + \left(\frac{x_j - A_0}{A_1} \right) \sqrt{1 - \left(\frac{A_0 - x_j}{A_1} \right)^2} \right\} \quad (84)$$

Application 2. Deriving Fourier Coefficients in Explicit Form

In the analysis of many communication circuits, an input signal $x(t) = A_0 + A_1 \cos \omega t$ is often applied to a memoryless nonlinearity $y = f(x)$ to obtain a periodic output [14]

$$y(t) = \alpha_0 + \sum_{k=1}^{\infty} \alpha_k \cos k\omega t \quad (85)$$

having only cosine components. The problem is to derive the Fourier coefficients $\alpha_0, \alpha_1, \dots, \alpha_k, \dots$ in a form that would provide some insight on the effect of the nonlinearities on the magnitude of these coefficients. A useful technique for doing this is given in [14] for several simple piecewise-linear curves. Since these curves are described graphically, the Fourier coefficients associated with each curve have to be derived on an ad hoc basis. Such tedious repetitions could be obviated by deriving a single formula with the help of our canonical piecewise-linear representation.

⁶Without loss of generality, we assume that $A_1 > |A_0 - x_j|$, for all $j = 1, 2, \dots, n$.

For simplicity, assume the piecewise-linear curve is continuous and can therefore be represented by

$$y = f(x) = a_0 + a_1 x + \sum_{j=1}^n b_j |x - x_j| \quad (86)$$

The output time function due to the input $x(t) = A_0 + A_1 \cos \omega t$ is therefore given by

$$y(t) = a_0 + a_1 (A_0 + A_1 \cos \omega t) + \sum_{j=1}^n b_j |A_0 + A_1 \cos \omega t - x_j| \quad (87)$$

Let us first observe that if $A_0 - x_j \geq A_1$ (resp., $A_0 - x_j \leq -A_1$) in (87), then $|A_0 + A_1 \cos \omega t - x_j| = A_0 + A_1 \cos \omega t - x_j$ (resp., $-(A_0 + A_1 \cos \omega t - x_j)$), which is a cosine wave with a dc component. On the other hand, if $|A_0 - x_j| < A_1$ for some j , then $|A_0 + A_1 \cos \omega t - x_j|$ is no longer sinusoidal. However, this waveform can always be decomposed into two wave-trains made up of sine-wave tips as shown in Fig. 8. Observe that the two wave-trains are uniquely identified by a single parameter

$$\theta_j \triangleq 2\phi_j \triangleq 2 \cos^{-1} \left(\frac{x_j - A_0}{A_1} \right), \quad (88)$$

called the conduction angle, where $0 < \phi_j < \pi$. Since Fourier coefficients of "sine-wave tip" wave-trains such as those shown in Figs. 8(b) and (c) and parameterized by the conduction angle $2\phi_j$ have been derived and are widely available either in tabular or graphical form [14], it is but logical to express the Fourier coefficients of $y(t)$ in terms of the Fourier coefficients of these "sine-wave tip" wave-trains. To derive this relationship, rewrite $y(t)$ as follow:

$$y(t) = a_0 + a_1 (A_0 + A_1 \cos \omega t) + \sum_{A_0 - x_i \geq A_1} b_i (A_0 + A_1 \cos \omega t - x_i) - \sum_{A_0 - x_k \leq -A_1} b_k (A_0 + A_1 \cos \omega t - x_k) + \sum_{|A_0 - x_j| < A_1} b_j |A_0 + A_1 \cos \omega t - x_j| \quad (89)$$

where the subscripts i , j , and k are understood to sum over all those components in (87) corresponding to the three cases $A_0 - x_i \geq A_1$, $A_0 - x_k \leq -A_1$, and $|A_0 - x_j| < A_1$, respectively. Now the last term in (89) can be written as follows:

$$\begin{aligned}
|A_0 + A_1 \cos \omega t - x_j| &= \sum_{\ell=0}^{\infty} \{p_{j\ell} \cos \ell \omega t + q_{j\ell} \cos \ell (\omega t + \pi)\} \\
&= \sum_{\ell, \text{even}} (p_{j\ell} + q_{j\ell}) \cos \ell \omega t + \sum_{\ell, \text{odd}} (p_{j\ell} - q_{j\ell}) \cos \ell \omega t \quad (90)
\end{aligned}$$

where $p_{j\ell}$ and $q_{j\ell}$ denote the ℓ th harmonic cosine Fourier coefficient of that sine-wave tip wave-train having a conduction angle equal to $2\phi_j$, and $2(\pi - \phi_j)$, respectively. Substituting (90) into (89) and collecting terms together, we obtain the following explicit formula:

$$\begin{aligned}
y(t) &= \left[a_0 + a_1 A_0 + \sum_{A_0 - x_i > A_1} b_i (A_0 - x_i) - \sum_{A_0 - x_k \leq -A_1} b_k (A_0 - x_k) + \sum_{|A_0 - x_j| < A_1} b_j (p_{j0} + q_{j0}) \right] \\
&+ \left[A_1 \left(a_1 + \sum_{A_0 - x_i > A_1} b_i - \sum_{A_0 - x_k \leq -A_1} b_k \right) + \sum_{|A_0 - x_j| < A_1} b_j (p_{j1} - q_{j1}) \right] \cos \omega t \\
&+ \sum_{\ell=2,4,6,\dots} \left[\sum_{|A_0 - x_j| < A_1} b_j (p_{j\ell} + q_{j\ell}) \right] \cos \ell \omega t \\
&+ \sum_{\ell=3,5,\dots} \left[\sum_{|A_0 - x_j| < A_1} b_j (p_{j\ell} - q_{j\ell}) \right] \cos \ell \omega t \quad (91)
\end{aligned}$$

Example 6. Consider a memory device whose TC plot is shown in Fig. 9(a).

Applying (13), we obtain the following piecewise-linear representation:

$$v_0 = T(v_1) = -\frac{7}{4} + \frac{1}{4} \left\{ |v_1 + 4| - |v_1 + 2| + 4|v_1| - 3|v_1 - 1| + |v_1 - 3| + |v_1 - 5| \right\} \quad (92)$$

The output waveform $v_0(t)$ due to the input $v_1(t) = 1 + 4\cos \omega t$ shown in Fig.

9(b) is obtained graphically and shown in Fig. 9(c). The Fourier coefficients of $v_0(t)$ could of course be obtained by any efficient computer techniques.

However, such a standard approach would not yield any qualitative information on the effect of the magnitude A_1 relative to the dc bias A_0 and the breakpoint locations. To apply (91), we first observe that the condition $|A_0 - x_i| < A_1$ is satisfied for this example only at the four breakpoints $v_1 = -2, 0, 1$, and 3 .

The corresponding conduction angles are therefore given by $2\phi_2 = 4.84$, $2\phi_3 = 3.64$, $2\phi_4 = \pi$, and $2\phi_5 = \frac{2}{3}\pi$ radians, respectively. The corresponding Fourier coefficients for $p_{j\ell}$ and $q_{j\ell}$ for the first five harmonics are then read off from the graph on p. 94 of [14] and tabulated as follows:

$P_{j\ell}$	$\ell=0$	1	2	3	4	5	$q_{j\ell}$	$\ell=0$	1	2	3	4	5
$P_{2\ell}$	2.94	3.71	0.238	-0.196	0.126	-0.056	$q_{2\ell}$	0.15	0.28	0.24	0.18	0.12	0.06
$P_{3\ell}$	1.80	2.45	0.80	-0.185	-0.09	0.09	$q_{3\ell}$	0.81	1.32	0.75	0.21	-0.096	-0.096
$P_{4\ell}$	1.32	1.92	0.88	0	-0.176	0	$q_{4\ell}$	1.32	1.92	0.88	0	-0.176	0
$P_{5\ell}$	0.44	0.75	0.55	0.29	0.056	-0.056	$q_{5\ell}$	2.4	3.0	0.54	-0.30	0.048	0.048

Substituting the parameters from (92) and the preceding table into (91) and simplifying, we obtain

$$y(t) = 1.3175 + 0.7225 \cos \omega t + 0.383 \cos 2\omega t - 0.1535 \cos 3\omega t \\ + 0.0425 \cos 4\omega t + 0.189 \cos 5\omega t \quad \blacksquare$$

The last two applications have been computational in nature. To demonstrate the usefulness of (13) for theoretical studies, our final example derives a new theorem on the existence and uniqueness of solutions.

Application 3. Deriving a new theorem on Existence and Uniqueness of Solution

The equilibrium equations for a large class of resistive nonlinear networks assumes the form [17]

$$\begin{bmatrix} g(v_a) \\ f(i_b) \end{bmatrix} - \begin{bmatrix} H_{aa} & H_{ab} \\ H_{ba} & H_{bb} \end{bmatrix} \begin{bmatrix} v_a \\ i_b \end{bmatrix} = \begin{bmatrix} s_a \\ s_b \end{bmatrix} \quad (93)$$

where $i_a = g(v_a)$ and $v_b = f(i_b)$ denote the constitutive relations of nonlinear voltage-controlled and current-controlled resistors, respectively, and where H_{jk} and s_j denote respectively the hybrid matrix and source vector of the linear n-port obtained by extracting all nonlinear resistors of the network. Now if we assume that all nonlinear resistors are uncoupled and characterized by a continuous piecewise-linear curve, then each component of $g(v_a)$ and $f(i_b)$ can be represented by (13) and (93) can be rewritten as follows:

$$P(x) \triangleq \begin{bmatrix} a_{01} \\ a_{02} \\ \vdots \\ a_{0m} \end{bmatrix} + \left\{ \begin{bmatrix} a_{11} & 0 & \dots & 0 \\ 0 & a_{12} & & 0 \\ \vdots & \vdots & \ddots & \vdots \\ 0 & \dots & & a_{1m} \end{bmatrix} - \begin{bmatrix} h_{11} & h_{12} & \dots & h_{1m} \\ h_{21} & h_{22} & \dots & h_{2m} \\ \vdots & \vdots & \ddots & \vdots \\ h_{m1} & h_{m2} & \dots & h_{mm} \end{bmatrix} \right\} \begin{bmatrix} x_1 \\ x_2 \\ \vdots \\ x_m \end{bmatrix} + \begin{bmatrix} \sum_{j=1}^b b_{1j} |x_1 - x_{1j}| \\ \sum_{j=1}^n b_{2j} |x_2 - x_{2j}| \\ \vdots \\ \sum_{j=1}^n b_{mj} |x_m - x_{mj}| \end{bmatrix} = \begin{bmatrix} s_1 \\ s_2 \\ \vdots \\ s_m \end{bmatrix} \quad (94)$$

We are now ready to state the following theorem:

Existence and Uniqueness Theorem

Any resistive nonlinear network characterized by (94) has a unique solution if, and only if, the matrix

$$M \triangleq \begin{bmatrix} a_{11} + b_{11}^T \varepsilon^{j_1} & 0 & \dots & 0 \\ 0 & a_{12} + b_{12}^T \varepsilon^{j_2} & & \\ \vdots & & \ddots & \\ 0 & \dots & \dots & a_{1m} + b_{1m}^T \varepsilon^{j_m} \end{bmatrix} - \begin{bmatrix} h_{11} & h_{12} & \dots & h_{1m} \\ h_{21} & h_{22} & \dots & h_{2m} \\ \dots & \dots & \dots & \dots \\ h_{m1} & h_{m2} & \dots & h_{mm} \end{bmatrix} \quad (95)$$

where $b_k \triangleq [b_{k1} \ b_{k2} \ \dots \ b_{kn}]^T$ and $\varepsilon^{j_k} = [1 \ 1 \ \dots \ \varepsilon \ -1 \ \dots \ -1]^T$ (where ε is located at the j_k th row) is non-singular for all j_1, j_2, \dots, j_m ranging from 1 to n , and for all $\varepsilon \in [-1, 1]$.

Proof. See Appendix D.

The point we wish to make with this example is that without resorting to the canonical representation (13), it would have been impossible to derive such an explicit necessary and sufficient condition as (95).

CONCLUDING REMARKS

The section-wise piecewise-linear representations presented in the preceding sections seem to be ideally suited for modeling nonlinear devices, circuits, and systems. The closed form canonical representations for $f(x)$ are global in the sense that they are valid for all values of $x \in \mathbb{R}^n$. The coefficients characterizing these representations can be calculated efficiently and the amount of computer storage space is minimal in the sense that only the characterizing coefficients need be stored. Since the canonical representations contain tensor-like product terms, they appear to be at least as accurate as the widely used multivariate approximation method employing tensor products [15]. However, the coefficients in our representations can be identified much more efficiently. Moreover, unlike other approximation methods, the "section-wise piecewise-linear" representations can allow finite jump discontinuities--a unique feature that should be useful for analyzing many circuit and control systems containing devices characterized by discontinuities characteristics such as zener diodes, relay, etc.

APPENDIX

A. Proof of Property 4.

Let m_k and \hat{m}_k be the slopes of $f(\cdot)$ and $f^{-1}(\cdot)$ corresponding to the interval I_k for $k = 0, 1, \dots, n$. Then

$$\hat{m}_k = \frac{1}{m_k} = \frac{1}{a_1 + \sum_{j=1}^n b_j - \sum_{j=k+1}^n b_j} \quad (\text{A.1})$$

$$\hat{a}_1 = \frac{1}{2} \left(\frac{1}{m_0} + \frac{1}{m_n} \right) = \frac{a_1}{a_1^2 - \left(\sum_{j=1}^n b_j \right)^2} \quad (\text{A.2})$$

$$\begin{aligned} \hat{b}_k &= \frac{1}{2} \left(\frac{1}{m_k} - \frac{1}{m_{k-1}} \right) \\ &= \frac{1}{2} \left(\frac{1}{a_1 + \sum_{j=1}^k b_j - \sum_{j=k+1}^n b_j} - \frac{1}{a_1 + \sum_{j=1}^{k-1} b_j - \sum_{j=k}^n b_j} \right) \\ &= - \frac{b_k}{\left(a_1 + \sum_{j=1}^{k-1} b_j - \sum_{j=k+1}^n b_j \right)^2 - b_k^2} \quad \text{for } k = 0, 1, \dots, n \end{aligned} \quad (\text{A.3})$$

Finally, from (61), we obtain

$$a_0 = f^{-1}(0) - \sum_{j=1}^n \hat{b}_j |f(x_j)| \quad \blacksquare$$

B. Proof of Property 5

Substituting (71) for x in (70), we obtain

$$\begin{aligned} f \circ g(z) &= a_0^f + a_1^f g(z) + \sum_{i=1}^{n_f} \left\{ b_i^f |g(z) - x_i| + c_i^f \operatorname{sgn}(g(z) - x_i) \right\} \\ &= a_0^f + a_1^f g(z) + \sum_{i=1}^{n_f} \left\{ b_i^f (g(z) - x_i) + c_i^f \right\} \operatorname{sgn}(g(z) - x_i) \\ &= a_0^f + a_1^f \left\{ a_0^g + a_1^g z + \sum_{j=1}^{n_g} (b_j^g |z - z_j| + c_j^g \operatorname{sgn}(z - z_j)) \right\} \\ &\quad + \sum_{i=1}^{n_f} \left\{ b_i^f \left[a_0^g + a_1^g z + \sum_{j=1}^{n_g} (b_j^g |z - z_j| + c_j^g \operatorname{sgn}(z - z_j)) - x_i \right] + c_i^f \right\} \operatorname{sgn}(g(z) - x_i) \end{aligned} \quad (\text{B.1})$$

Since the function $g(\cdot)$ is strictly increasing by assumption, we can write

$$\operatorname{sgn}(g(z)-x_i) = \operatorname{sgn}(z-z_i^*) \quad (\text{B.2})$$

where z_i^* is the solution of $g(z) - x_i = 0$.

From (B.1) and (B.2) we obtain

$$\begin{aligned} f \circ h(z) = & a_0^f + a_1^f a_0^g + a_1^f a_1^g z + \sum_{j=1}^n a_1^f b_j^g |z-z_j| + \sum_{j=1}^n a_1^f c_j^g \operatorname{sgn}(z-z_j) \\ & + \sum_{i=1}^{n_f} \left\{ b_i^f (a_0^g - x_i) + c_i^f \right\} \operatorname{sgn}(z-z_i^*) + \sum_{i=1}^{n_f} b_i^f a_1^g z \operatorname{sgn}(z-z_i^*) \\ & + \sum_{i=1}^{n_f} b_i^f \sum_{j=1}^n b_j^g |z-z_j| \operatorname{sgn}(z-z_i^*) + \sum_{i=1}^{n_f} b_i^f \left\{ \sum_{j=1}^n [c_j^g \operatorname{sgn}(z-z_j)] \operatorname{sgn}(z-z_i^*) \right\} \quad (\text{B.3}) \end{aligned}$$

The three piecewise-linear functions $z \operatorname{sgn}(z-z_i)$, $|z-z_j| \operatorname{sgn}(z-z_i^*)$ and $\operatorname{sgn}(z-z_j) \operatorname{sgn}(z-z_i^*)$ in (B.3) can be rewritten as follows:

$$z \operatorname{sgn}(z-z_i) = |z-z_i^*| + z_i^* \operatorname{sgn}(z-z_i^*) \quad (\text{B.4})$$

$$\begin{aligned} |z-z_j| \operatorname{sgn}(z-z_i^*) = & -z_j + z + \operatorname{sgn}(z_j-z_i^*) |z-z_j| - \operatorname{sgn}(z_j-z_i^*) |z-z_i^*| \\ & + |z_j-z_i^*| \operatorname{sgn}(z-z_i^*) \quad (\text{B.5}) \end{aligned}$$

and

$$\operatorname{sgn}(z-z_j) \operatorname{sgn}(z-z_i^*) = 1 + \operatorname{sgn}(z_j-z_i^*) \operatorname{sgn}(z-z_j) - \operatorname{sgn}(z_j-z_i^*) \operatorname{sgn}(z-z_i^*) \quad (\text{B.6})$$

Hence (72) follows from (B.3)-(B.6). \blacksquare

C. Derivation of Describing Functions $D_0(A_0, A_1)$ and $D_1(A_0, A_1)$.

Substituting (82) for $f(\cdot)$ in (80), we obtain

$$\begin{aligned} D_0 = & \frac{1}{2\pi} \int_0^{2\pi} \left\{ a_0 + a_1 A_0 + a_1 A_1 \cos \phi + \sum_{j=1}^n (b_j (A_0 - x_j) + c_j + b_j A_1 \cos \phi) \right. \\ & \left. \cdot \operatorname{sgn}(A_0 - x_j + A_1 \cos \phi) \right\} d\phi \\ = & a_0 + a_1 A_0 + \frac{1}{2\pi} \sum_{j=1}^n \left\{ \int_0^{2\pi} (b_j (A_0 - x_j) + c_j + b_j A_1 \cos \phi) d\phi \right. \\ & \left. - 2 \int_{\phi_j}^{2\pi - \phi_j} (b_j (A_0 - x_j) + c_j + b_j A_1 \cos \phi) d\phi \right\} \quad (\text{C.1}) \end{aligned}$$

where $\phi_j \triangleq \cos^{-1}\left(\frac{x_j - A_0}{A_1}\right)$, $\phi_j \in (0, \pi)$

The angle ϕ_j is well-defined since $|A_0 - x_j| < A_1$ by assumption.

Now observe that

$$\frac{1}{2\pi} \int_0^{2\pi} (b_j(A_0 - x_j) + c_j + b_j A_1 \cos \phi) d\phi = b_j(A_0 - x_j) + c_j \quad (C.2)$$

and

$$\begin{aligned} \frac{1}{\pi} \int_{\phi_j}^{2\pi - \phi_j} (b_j(A_0 - x_j) + c_j + b_j A_1 \cos \phi) d\phi &= \frac{1}{\pi} \left[(b_j(A_0 - x_j) + c_j) \phi + b_j A_1 \sin \phi \right]_{\phi_j}^{2\pi - \phi_j} \\ &= \frac{1}{\pi} \left[(b_j(A_0 - x_j) + c_j) (2\pi - 2\phi_j) + b_j A_1 (\sin(2\pi - \phi_j) - \sin \phi_j) \right] \\ &= \frac{2}{\pi} \left\{ [b_j(A_0 - x_j) + c_j] \left[\pi - \cos^{-1}\left(\frac{x_j - A_0}{A_1}\right) \right] - b_j \sqrt{A_1^2 - (A_0 - x_j)^2} \right\} \end{aligned} \quad (C.3)$$

It follows from (C.1)-(C.3) that

$$D_0 = a_0 + a_1 A_0 + \frac{2}{\pi} \sum_{j=1}^n \left\{ [b_j(A_0 - x_j) + c_j] \left[\cos^{-1}\left(\frac{A_0 - x_j}{A_1}\right) - \frac{\pi}{2} \right] + b_j \sqrt{A_1^2 - (A_0 - x_j)^2} \right\} \quad (83)$$

Next substituting (82) for $f(\cdot)$ in (81), we obtain

$$\begin{aligned} D_1 &= \frac{1}{\pi A_1} \int_0^{2\pi} \left\{ a_0 + a_1 A_0 + a_1 A_1 \cos \phi + \sum_{j=1}^n [b_j(A_0 - x_j) + c_j + b_j A_1 \cos \phi] \right. \\ &\quad \left. \cdot \operatorname{sgn}(A_0 - x_j + A_1 \cos \phi) \right\} \cos \phi d\phi \\ &= \frac{1}{\pi A_1} \left\{ a_1 A_1 \pi + \sum_{j=1}^n [b_j A_1 \pi - 2 \int_{\phi_j}^{2\pi - \phi_j} (b_j(A_0 - x_j) + c_j + b_j A_1 \cos \phi) \cdot \cos \phi d\phi] \right\} \\ &= a_1 + \sum_{j=1}^n \left\{ b_j - \frac{2}{\pi A_1} \left(\left[(b_j(A_0 - x_j) + c_j) \sin \phi \right]_{\phi_j}^{2\pi - \phi_j} + b_j A_1 \int_{\phi_j}^{2\pi - \phi_j} \cos^2 \phi d\phi \right) \right\} \\ &= a_1 + \sum_{j=1}^n \left\{ b_j - \frac{2}{\pi A_1} \left[(b_j(A_0 - x_j) + c_j) (-2 \sin \phi_j) + \frac{b_j A_1}{2} (2\pi - 2\phi_j - \sin 2\phi_j) \right] \right\} \\ &= a_1 + \sum_{j=1}^n \left\{ b_j + \frac{4}{\pi A_1} [b_j(A_0 - x_j) + c_j] \sqrt{1 - \left(\frac{A_0 - x_j}{A_1}\right)^2} \right. \\ &\quad \left. + \frac{2b_j}{\pi} \left[\cos^{-1}\left(\frac{x_j - A_0}{A_1}\right) - \pi + \frac{x_j - A_0}{A_1} \sqrt{1 - \left(\frac{A_0 - x_j}{A_1}\right)^2} \right] \right\} \quad (84) \end{aligned}$$

D. Proof of Existence and Uniqueness Theorem

The proof follows from a theorem by Fujisawa and Kuh on homeomorphism [23], namely,

" $p(x)$ is a homeomorphism of \mathbb{R}^m onto itself if, and only if, for any unit vector α and for any $x \in \mathbb{R}^m$, there exists one and only one nonzero vector $\beta = \hat{\beta}(\alpha, x)$ such that $p(x+v\beta) = p(x) + v\alpha$ for all sufficiently small positive v ."

It follows from (94) that

$$p(x+v\beta) - p(x) = v \left\{ \begin{bmatrix} a_{11} & 0 & \dots & 0 \\ 0 & a_{12} & & \\ \vdots & & \ddots & \\ 0 & \dots & & a_{1m} \end{bmatrix} - \begin{bmatrix} h_{11} & h_{12} & \dots & h_{1m} \\ \vdots & \vdots & & \vdots \\ \vdots & \vdots & & \vdots \\ h_{m1} & h_{m2} & \dots & h_{mn} \end{bmatrix} \right\} \beta + \left[\begin{array}{l} \sum_{j=1}^n b_{1j} (|x_1 + v\beta_1 - x_{1j}| - |x_1 - x_{1j}|) \\ \sum_{j=1}^n b_{2j} (|x_2 + v\beta_2 - x_{2j}| - |x_2 - x_{2j}|) \\ \vdots \\ \sum_{j=1}^n b_{mj} (|x_m + v\beta_m - x_{mj}| - |x_m - x_{mj}|) \end{array} \right] \quad (D.1)$$

Observe that $|x_k + v\beta_k - x_{kj}| - |x_k - x_{kj}| = v\beta_k S_{kj}(x_k, \beta_k)$, where $S_{kj}(x_k, \beta_k)$ is a piecewise-linear function as shown in Fig. A-1. So long as $v > 0$ is sufficiently small such that both x_{kj} and $x_{kj} - v\beta_k$ belong to the same segment for all $j = 1, 2, \dots, n$, then the term $\sum_{j=1}^n b_{kj} (|x_k + v\beta_k - x_{kj}| - |x_k - x_{kj}|) =$

$$v\beta_k \sum_{j=1}^n b_{kj} S_{kj}(x_k, \beta_k) \text{ becomes } v\beta_k \sum_{j=1}^{\ell-1} b_{kj} + \epsilon b_{k\ell} - \sum_{j=\ell+1}^n b_{kj}, \quad \epsilon \in [-1, 1] \quad (D.2)$$

whenever x_k belongs to the interval between $x_{k\ell}$ and $x_{k\ell} - v\beta_k$. Hence if we let $\epsilon^{jk} \triangleq (1 \ 1 \ \dots \ \epsilon \ -1 \ \dots \ -1)^T$ where ϵ is located at the jk^{th} position, then (D.2) can be rewritten as $v\beta_k b_{k\ell}^T \epsilon^{jk}$, where $jk = \ell$. Combining (D.1) and (D.2),

we obtain

$$p(x+v\beta) - p(x) = v \left\{ \begin{bmatrix} a_{11} & 0 & \dots & 0 \\ 0 & a_{12} & & 0 \\ \vdots & & \ddots & \\ 0 & \dots & & a_{1n} \end{bmatrix} - \begin{bmatrix} h_{11} & \dots & h_{1m} \\ h_{21} & \dots & h_{2m} \\ \vdots & & \vdots \\ h_{m1} & \dots & h_{mm} \end{bmatrix} \right\} \beta + v \begin{bmatrix} b_1^T \epsilon^j & 1 & 0 & \dots & 0 \\ 0 & b_2^T \epsilon^j & & & \\ \vdots & & \ddots & & \\ 0 & \dots & & b_m^T \epsilon^j & \end{bmatrix} \beta \quad (D.4)$$

Now in order for one, and only one, nonzero vector β to exist such that $p(\underline{x} + v\beta) - p(\underline{x}) = v\alpha$ for all sufficiently small $v > 0$, (95) must be non-singular for all unit vectors α and for all $\underline{x} \in \mathbb{R}^m$. Now if $\beta_k = 0$ for some \underline{x} and α , then we can find another \underline{x} with the same β_k and another α such that $\beta_k \neq 0$. Hence it is necessary that the matrix M in (95) be nonsingular for all j_1, j_2, \dots, j_m ranging from 1 to n and for all $\epsilon \in [-1, 1]$. If this condition is satisfied, then for all unit vectors α and for all $\underline{x} \in \mathbb{R}^m$, there exists a unique β and hence (94) has a unique solution. \blacksquare

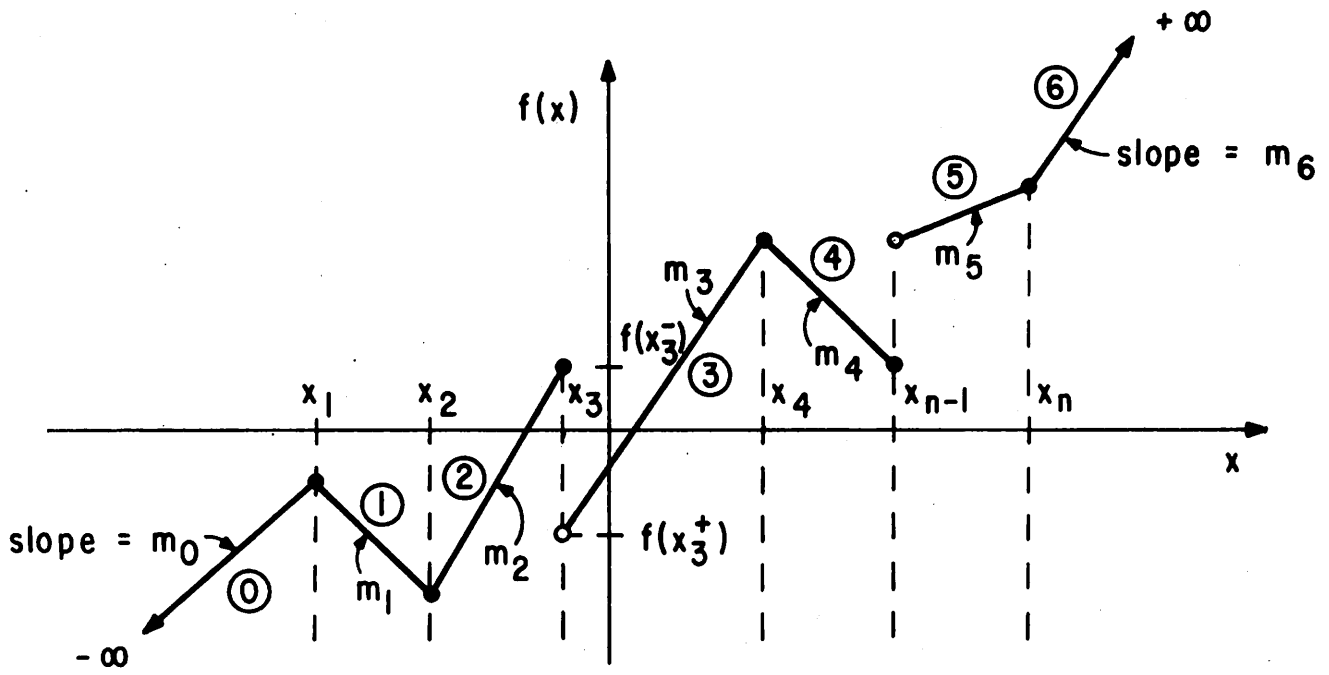
REFERENCES

1. J. F. P. Hudson, Piecewise-Linear Topology, New York: W. A. Benjamin, 1969.
2. K. S. Cole, Membranes, Ions and Impulses, Berkeley: University of California Press, 1972.
3. E. Schmidt, Thermodynamics, New York: Dover, 1966.
4. M. Iri, Network Flow, Transportation and Scheduling, New York: Academic Press, 1969.
5. J. B. Dennis, Mathematical Programming and Electrical Networks, New York: John Wiley, 1959.
6. A. A. Andronov, A. A. Vitt, and S. E. Khaikin, Theory of Oscillators, New York: Pergamon Press, 1966.
7. O. C. Zienkiewicz, The Finite Element Method in Engineering Science, New York: McGraw-Hill, 1971.
8. Dan Hartog, Mechanics, New York: Dover, 1948.
9. G. Rich, Hydraulic Transients, New York: Dover, 1962.
10. I. Flügge-Lötz, Discontinuous and Optimal Control, New York: McGraw-Hill, 1948.
11. H. J. Zimmerman and S. J. Mason, Electronic Circuit Theory, New York: John Wiley, 1959.
12. L. O. Chua, Introduction to Nonlinear Network Theory, New York: McGraw-Hill, 1969.
13. T. E. Stern, Theory of Nonlinear Networks and Systems, An Introduction, Reading, Mass.: Addison-Wesley, 1965.
14. K. K. Clarke and D. T. Hess, Communication Circuits: Analysis and Design, Reading, Mass.: Addison-Wesley, 1971.
15. J. R. Rice, The Approximation of Functions, Vol. II - Advanced Topics, Reading, Mass.: Addison Wesley, 1969.
16. J. H. Ahlberg, E. N. Nilson, and J. L. Walsh, Theory and Applications of Spline Functions, New York: Academic Press, 1967.
17. L. O. Chua and P-M Lin, Computer-Aided Analysis of Electronic Circuits: Algorithms and Computational Techniques, Englewood Cliffs, N.J.: Prentice-Hall, 1975.
18. L. O. Chua and S. M. Kang, "Memristive Devices and Systems," Proc. of the IEEE, Vol. 64, No. 2, Feb. 1976, pp. 209-223.

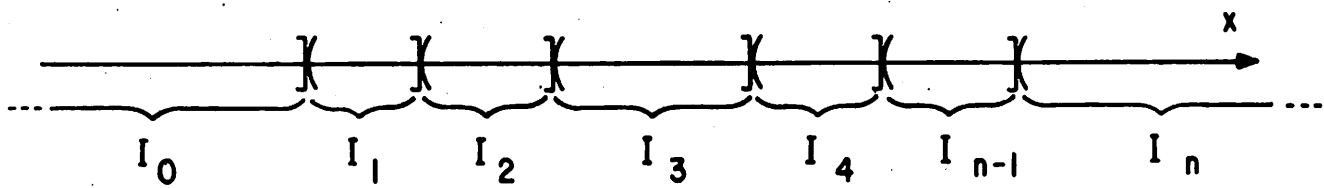
19. L. O. Chua and R. J. Schilling, "An Algorithm for Modeling the Sinusoidal Input/Steady State Response Behavior of Nonlinear Systems over a Set of Frequencies and Amplitudes," J. Franklin Institute, vol. 298, no. 2, pp. 101-124, Aug. 1974.
20. B. D. Wedlock and J. K. Roberge, Electronic Components and Measurements, Englewood Cliffs, N.J.: Prentice-Hall, 1969.
21. P. J. Davis, Interpolation and Approximation, New York: Blaisdell, 1963.
22. L. O. Chua, "Modeling of Three-Terminal Devices: A Black-Box Approach," IEEE Trans. on Circuit Theory, vol. CT-19, no. 6, Nov. 1972, pp. 555-562.
23. T. Fujisawa and E. S. Kuh, "Piecewise-linear Theory of Nonlinear Networks," SIAM Journal on Applied Mathematics, vol. 22, March 1972, pp. 307-328.

FIGURE CAPTIONS

- Fig. 1 A typical piecewise-linear curve with finite jump discontinuities and the intervals $I_j = (x_j, x_{j+1}]$ where the function is linear.
- Fig. 2 A Piecewise-linear curve with two finite jump discontinuities (Example 1).
- Fig. 3 The dc characteristics of a typical SCR is shown in (a) and modeled by the family of piecewise-linear curves shown in (b). The $(2n+2)$ model functions are shown in (c) through (1).
- Fig. 4 A simple multivalued "ideal diode" v - i curve is shown in (a) while a more complex unicursal multivalued curve is shown in (b), along with an arbitrarily chosen breakpoint $Q(x_6, y_6)$ as the parametric origin and an arbitrarily chosen orientation as indicated by arrow heads on the curve.
- Fig. 5 The unicursal multivalued piecewise-linear curve in (a) for Example 3 is represented by two single-valued piecewise-linear curves $v=v(\rho)$ and $i=i(\rho)$ shown respectively in (b) and (c).
- Fig. 6 The points shown in the cubical lattice in (a) are chosen as the set S of data points for the function defined by (46) of Example 4. The piecewise-linear curve $f(x_1, 0, 0)$ shown in (b) gives the values of the function $f(\cdot, x_1, x_2)$ over the cross-section $x_1=0$, $x_2=0$. The model function $a_0(x_2, x_3)$ shown in (c) has one less variable and is piecewise-linear along the cross sections $x_3=0, 1$, and 2.
- Fig. 7 The two resistors in the nonlinear voltage divider in (a) are characterized by the piecewise-linear curve shown in (c) and (d). The v_0 -vs.- v_i TC plot given by (78) is shown in (b).
- Fig. 8 The periodic waveform $p(t) = |A_0 + A_1 \cos \omega t - x_j|$ shown in (a) can always be decomposed into the two wave-trains $p_1(t)$ and $p_2(t)$ shown respectively in (b) and (c). Each wave-train is uniquely specified by its conduction angle $\theta_j \triangleq 2\phi_j \triangleq 2 \cos^{-1} \left(\frac{x_j - A_0}{A_1} \right)$.
- Fig. 9 The output waveform $v_0(t)$ shown in (c) is obtained by a graphical composition between the v_0 -vs.- v_i TC plot shown in (a) with the input waveform $v_i(t) = 1 + 4 \cos \omega t$ shown in (b). The unit-slope line in (d) is used for graphical construction.
- Fig. A-1 The graphs for $S_{kj}(x_k, \beta_k)$ for $\beta_k \geq 0$ in (a) and $\beta_k < 0$ in (b).



(a)



(b)

Fig. 1

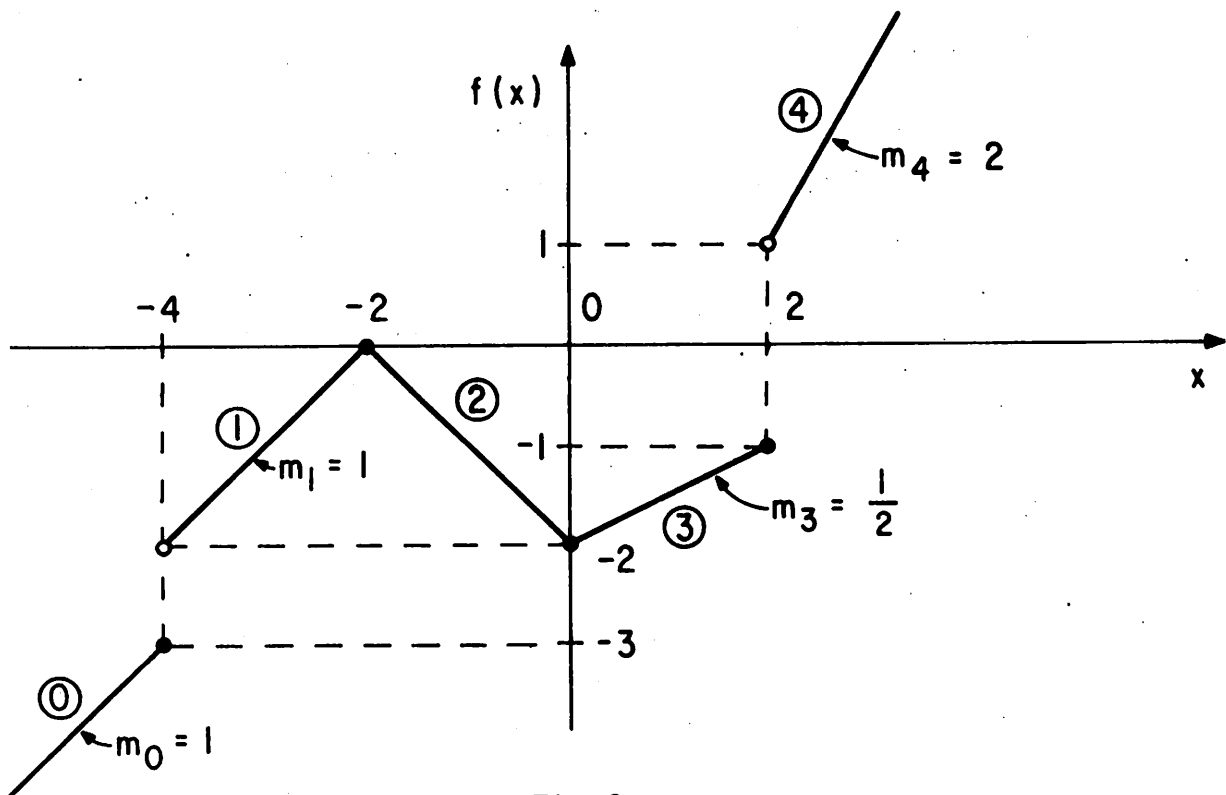
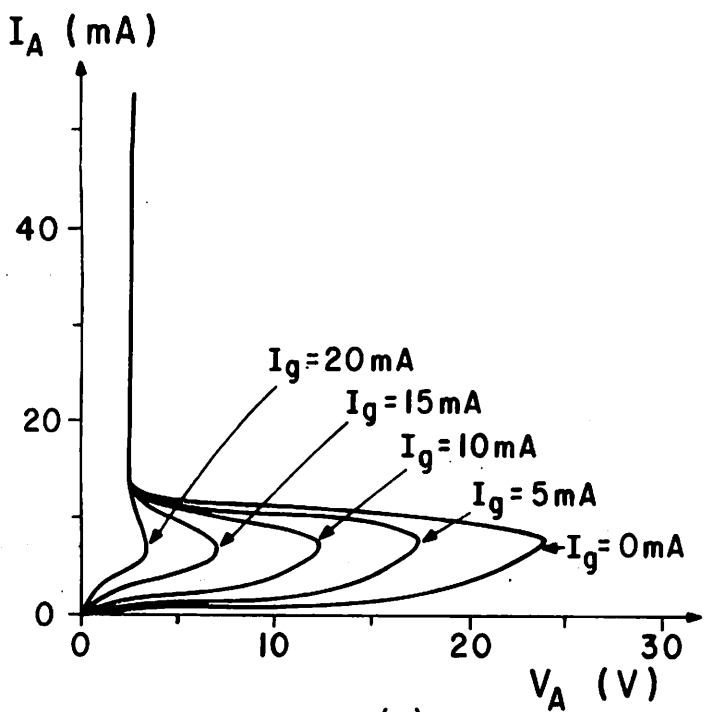
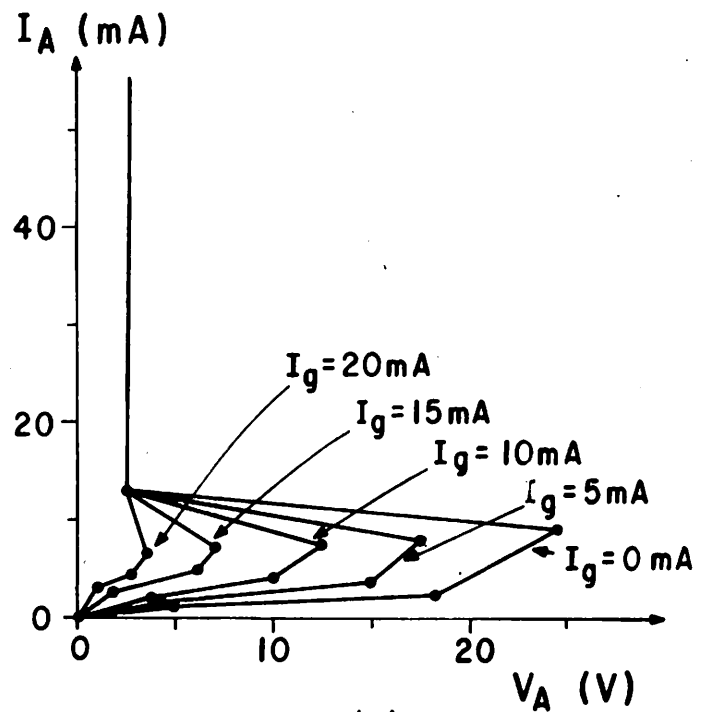


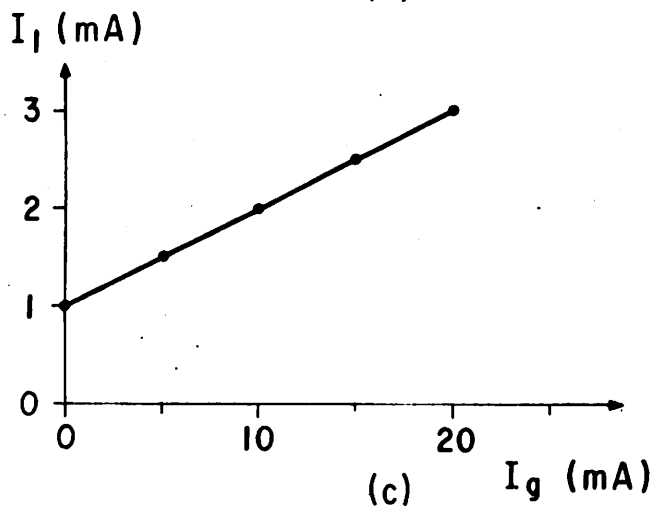
Fig. 2



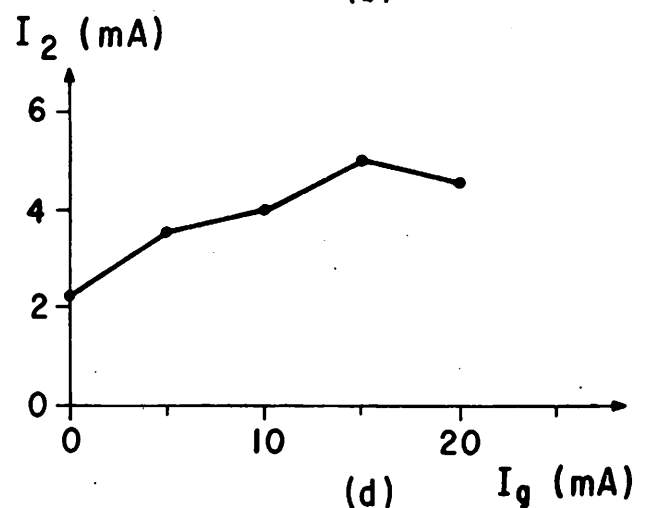
(a)



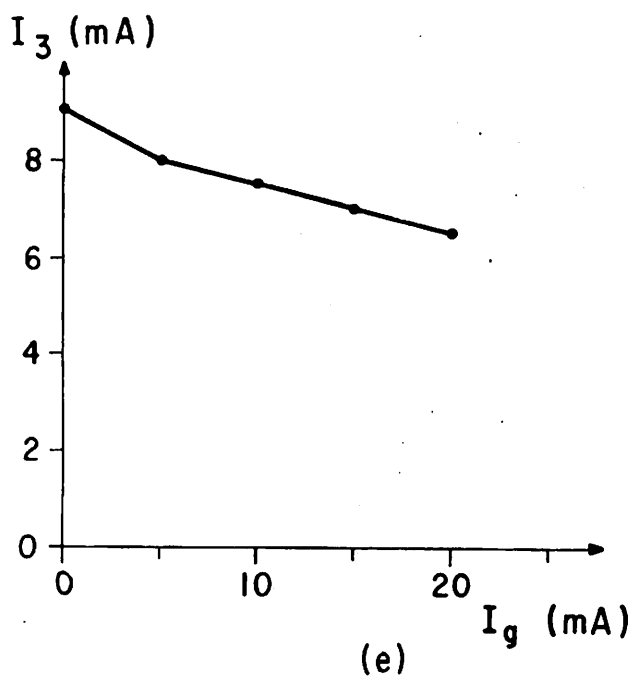
(b)



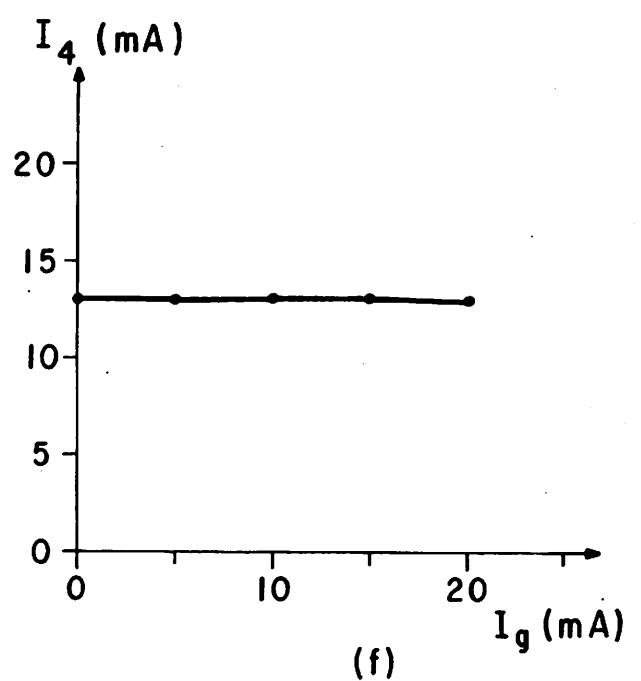
(c)



(d)



(e)



(f)

Fig. 3

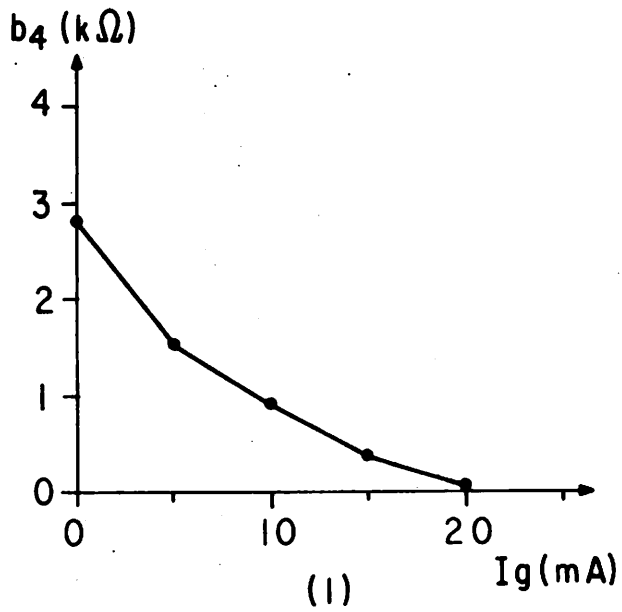
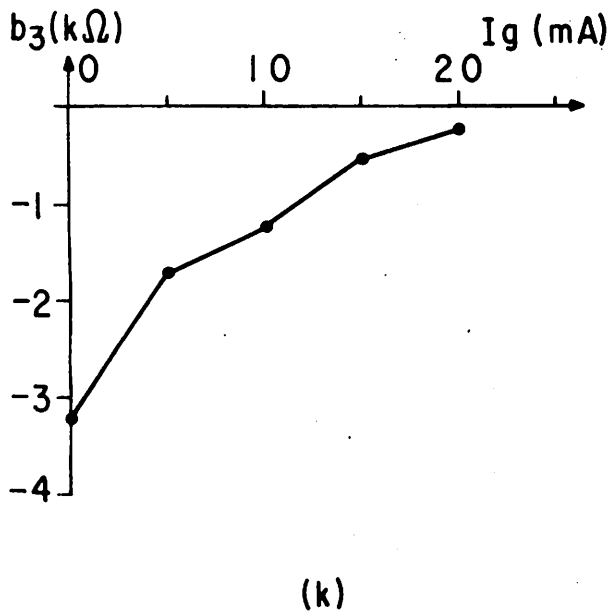
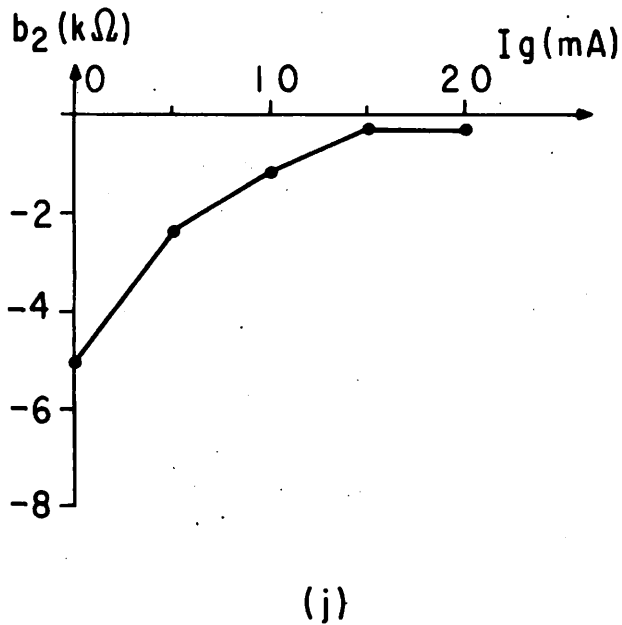
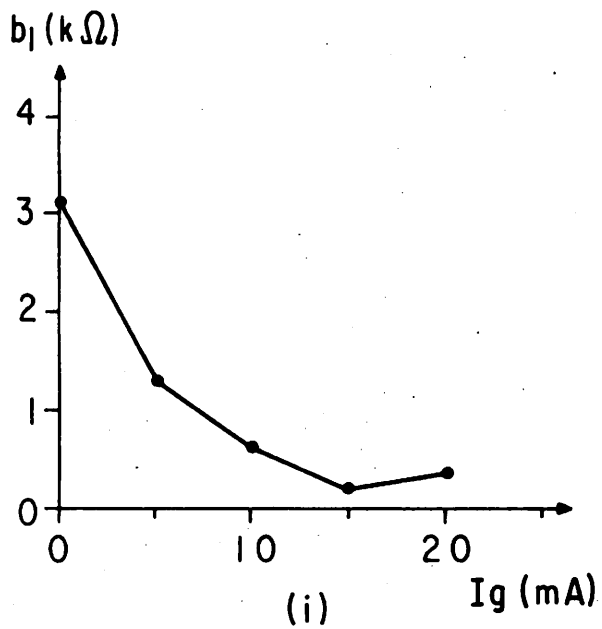
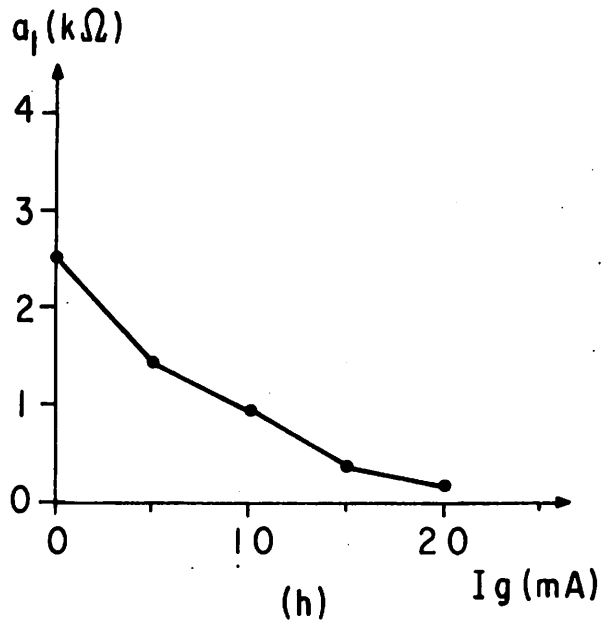
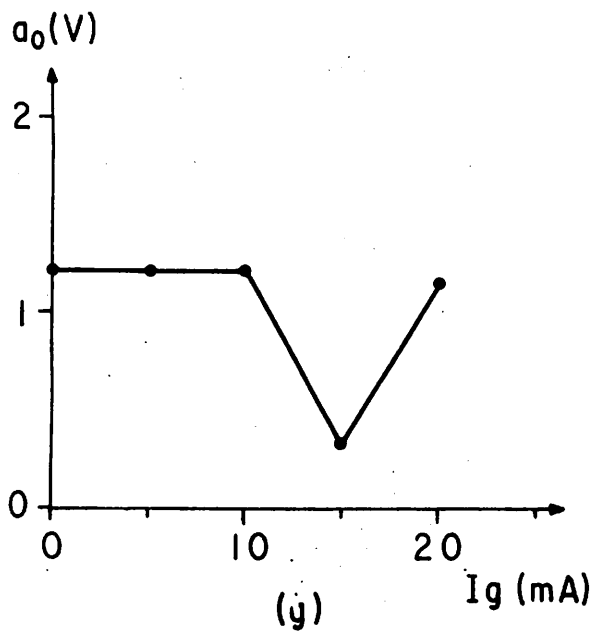
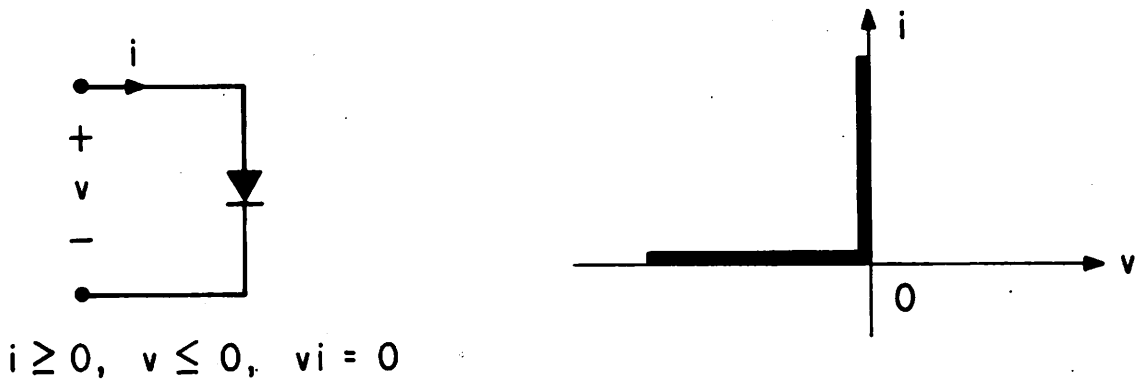
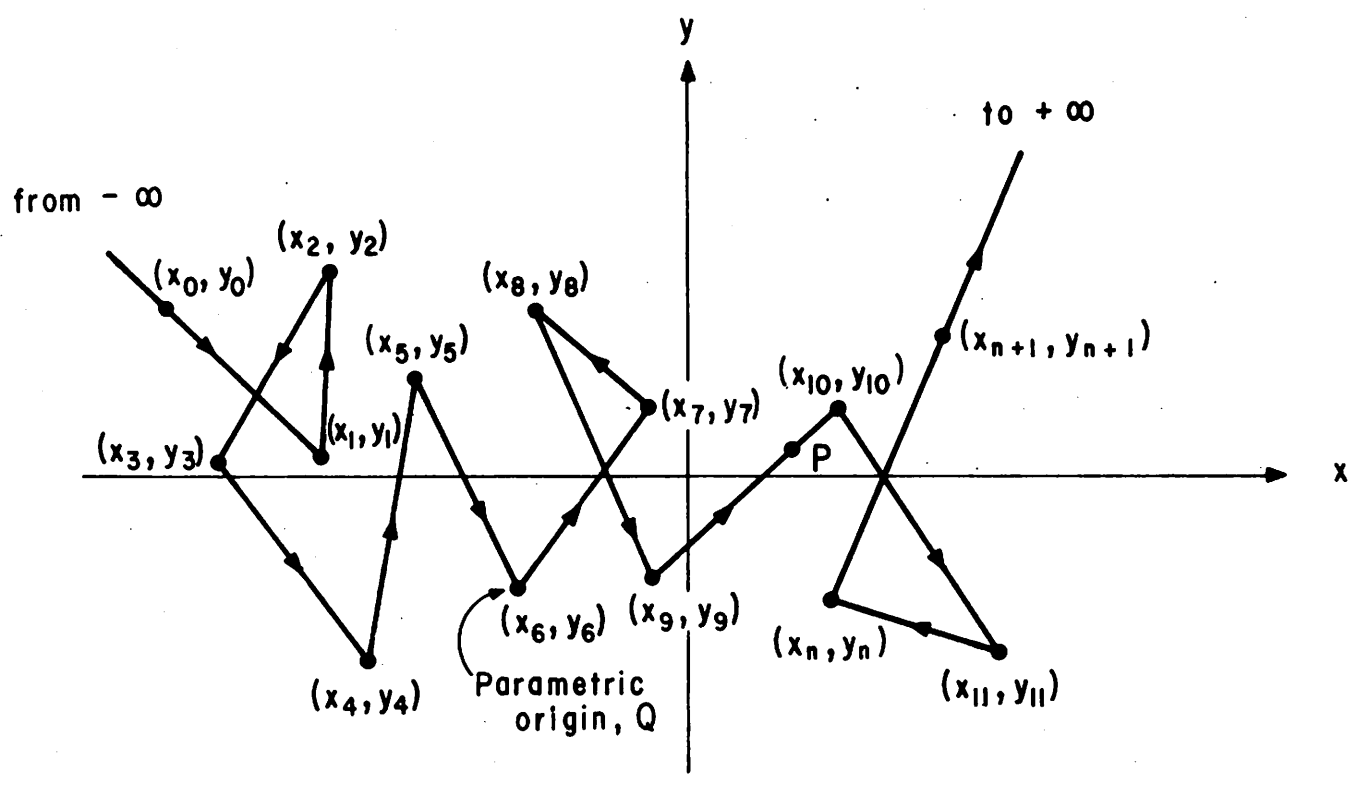


Fig. 3 (continued)



(a)



(b)

Fig. 4

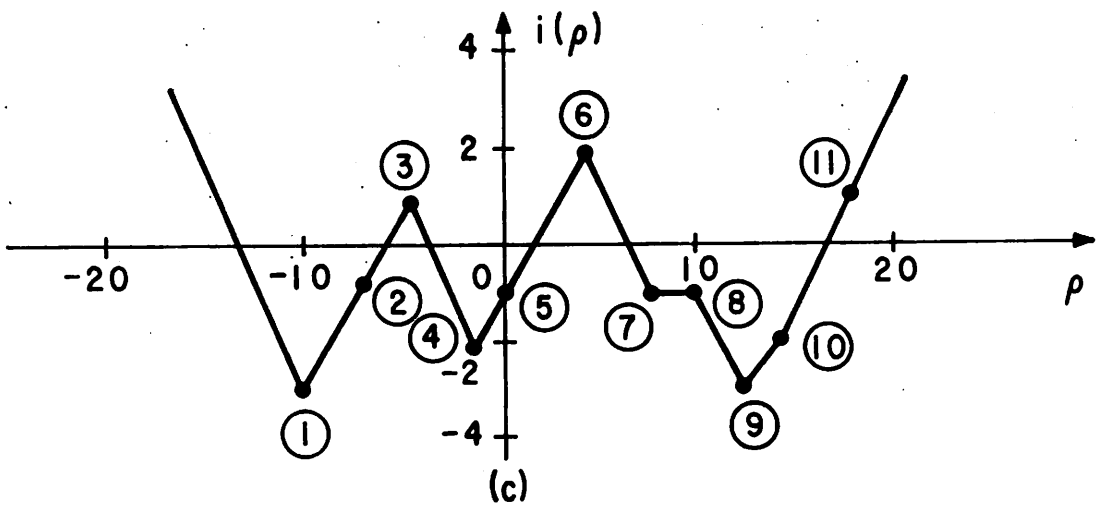
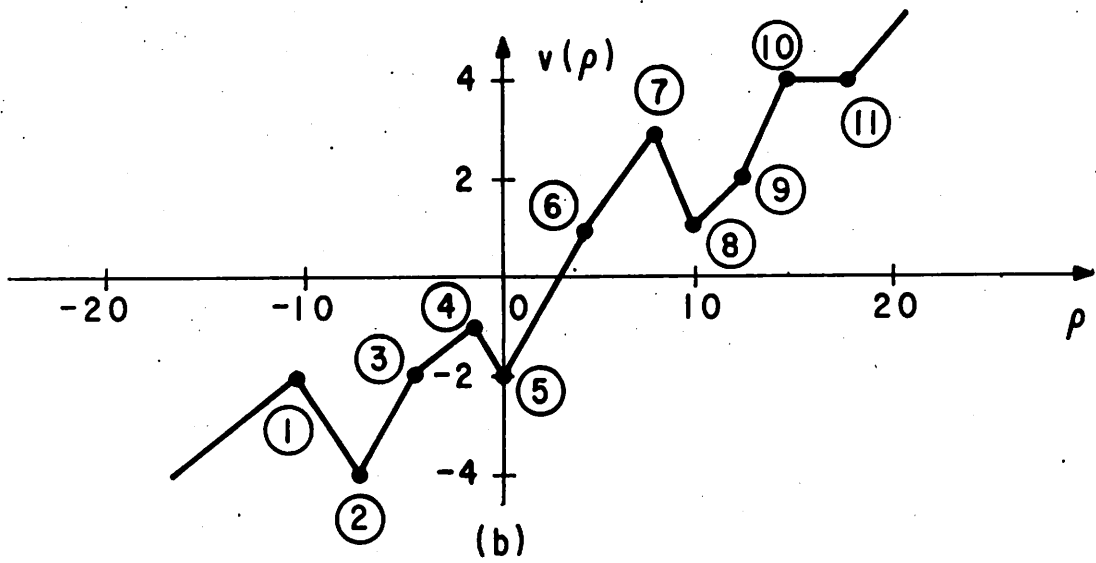
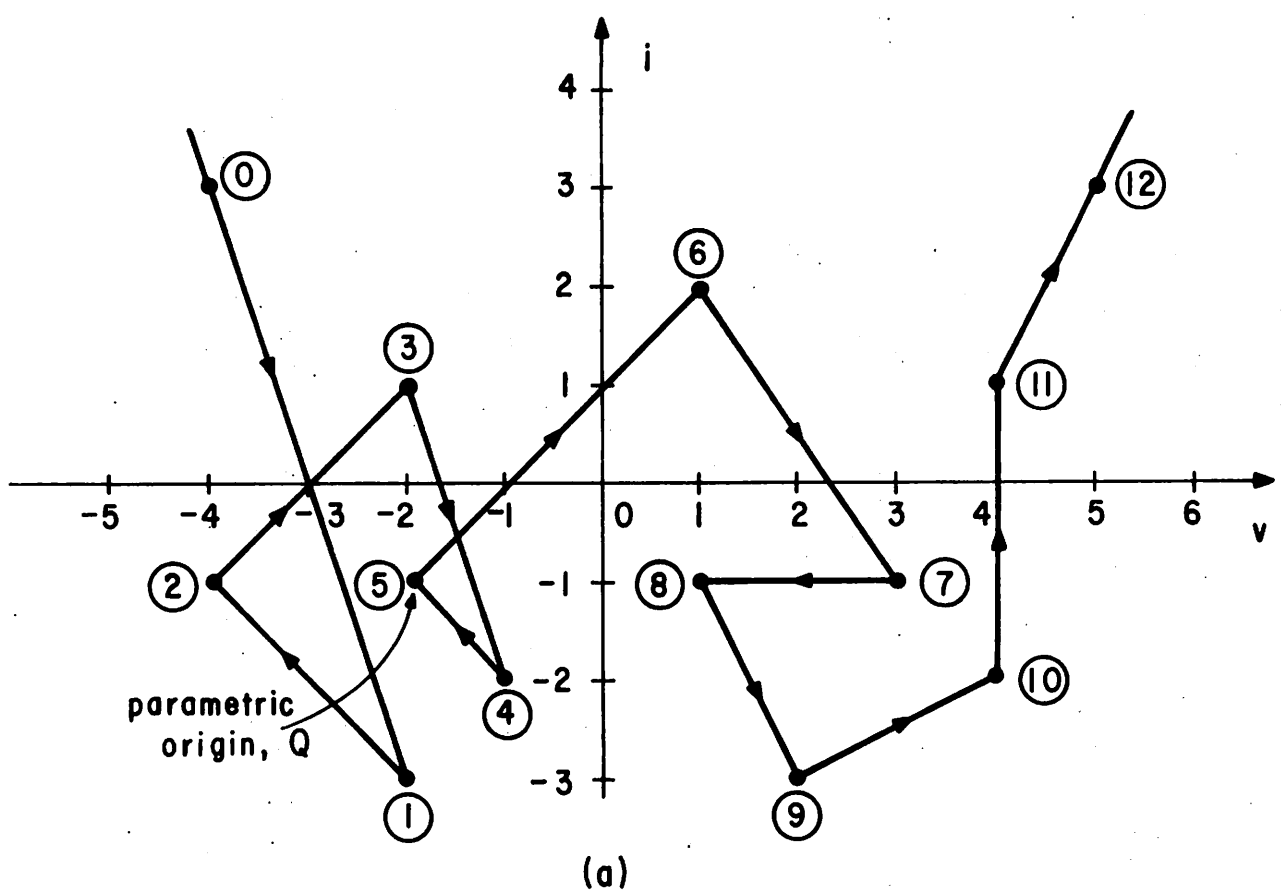
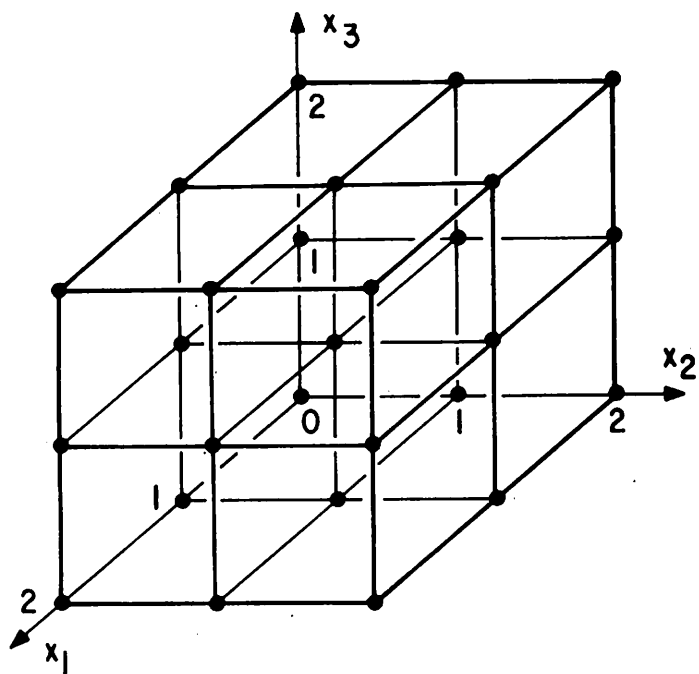
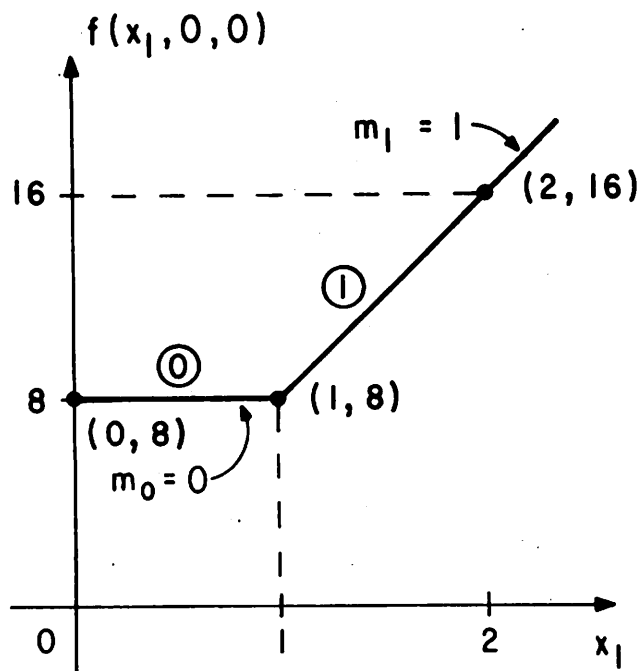


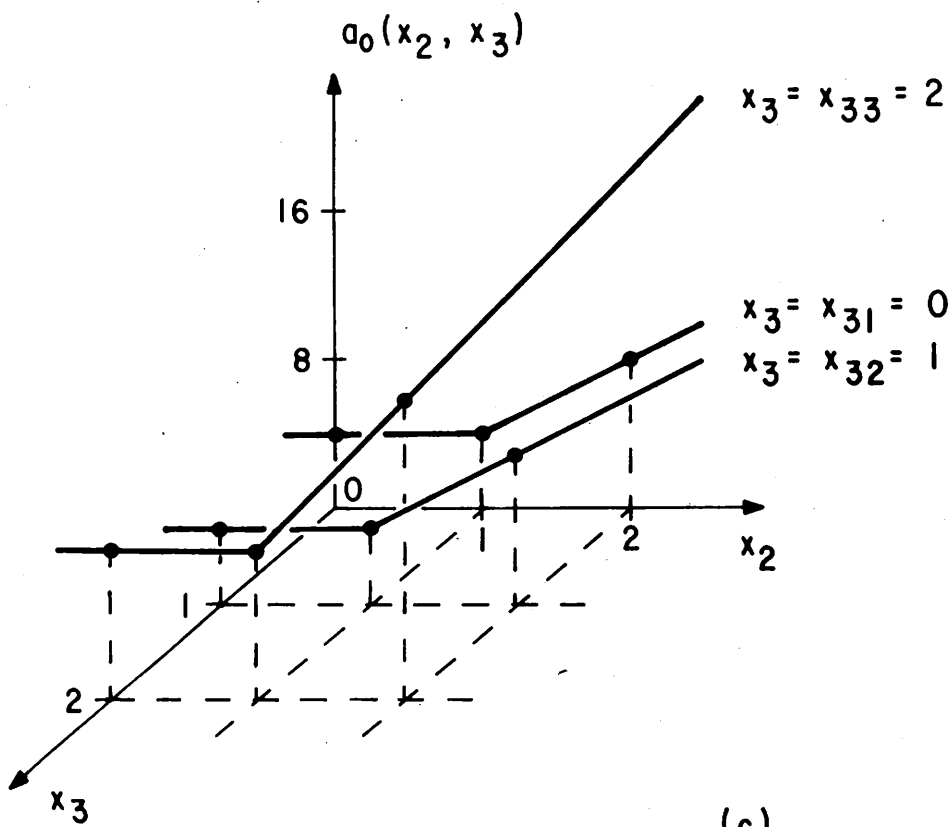
Fig. 5



(a).



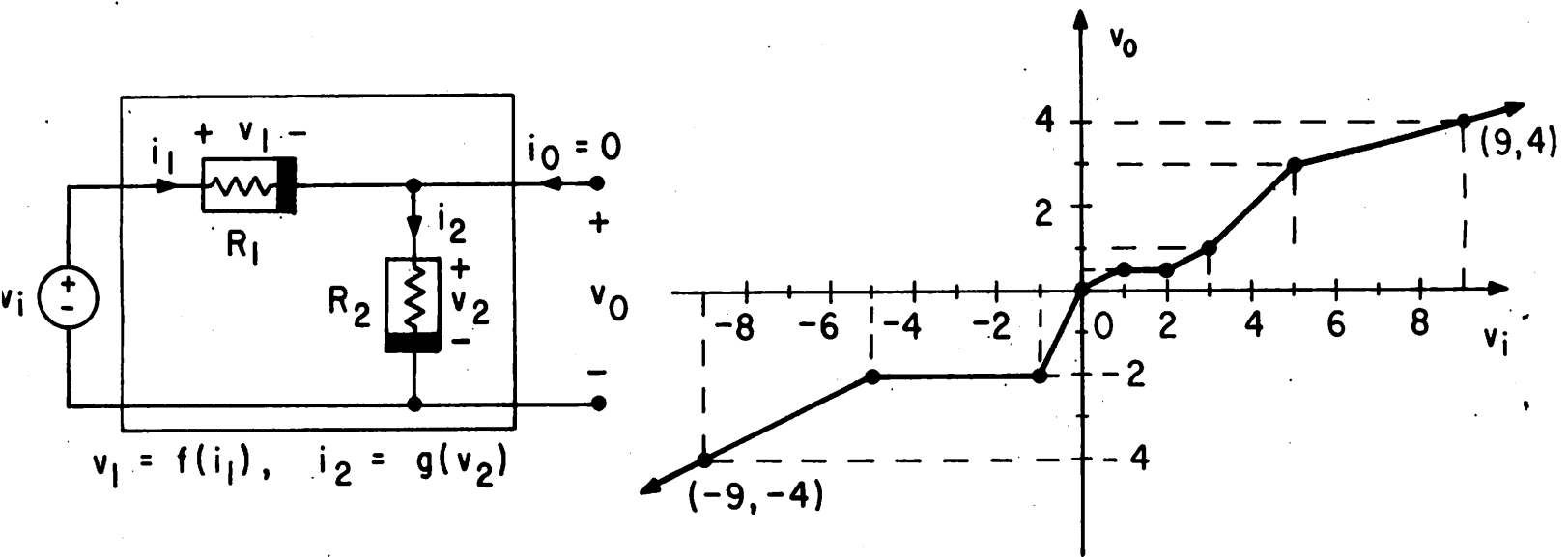
(b).



(c).

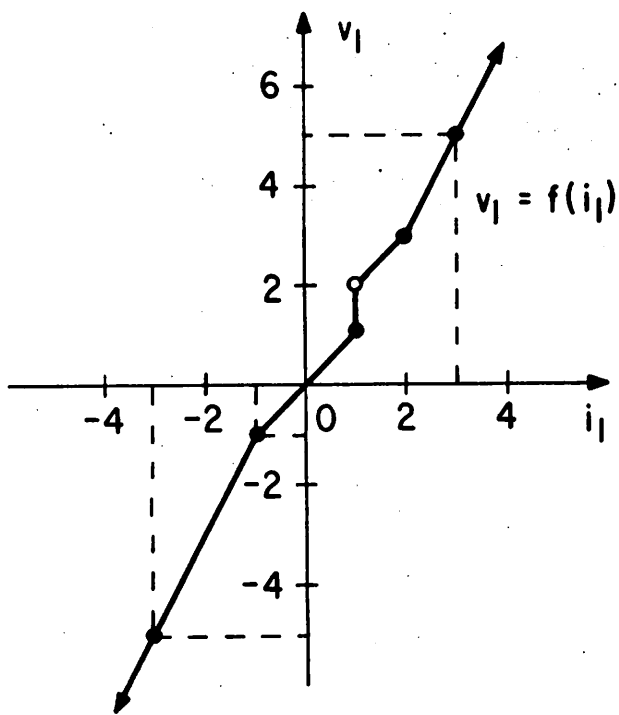
$x_3 \backslash x_2$	0	1	2
0	4	4	8
1	4	4	8
2	8	8	16

Fig. 6

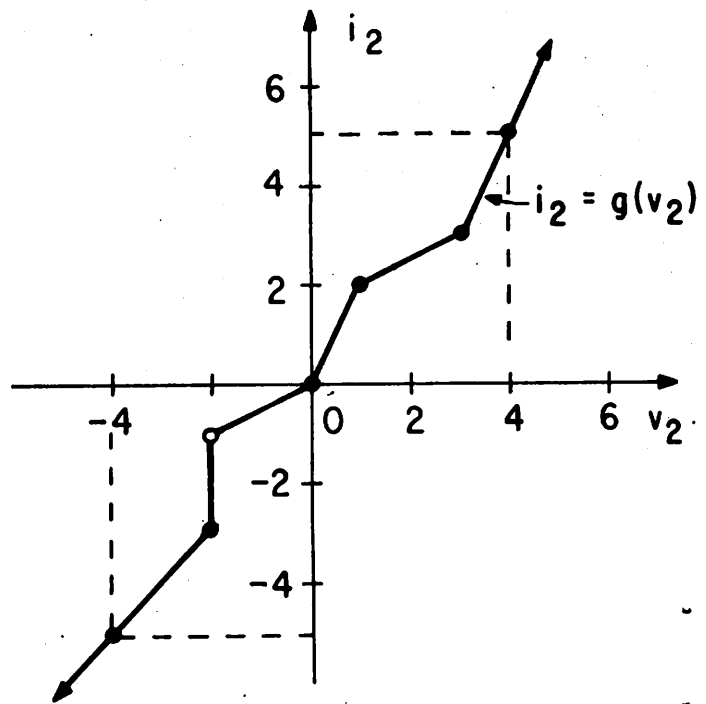


(a)

(b)



(c)



(d)

Fig. 7

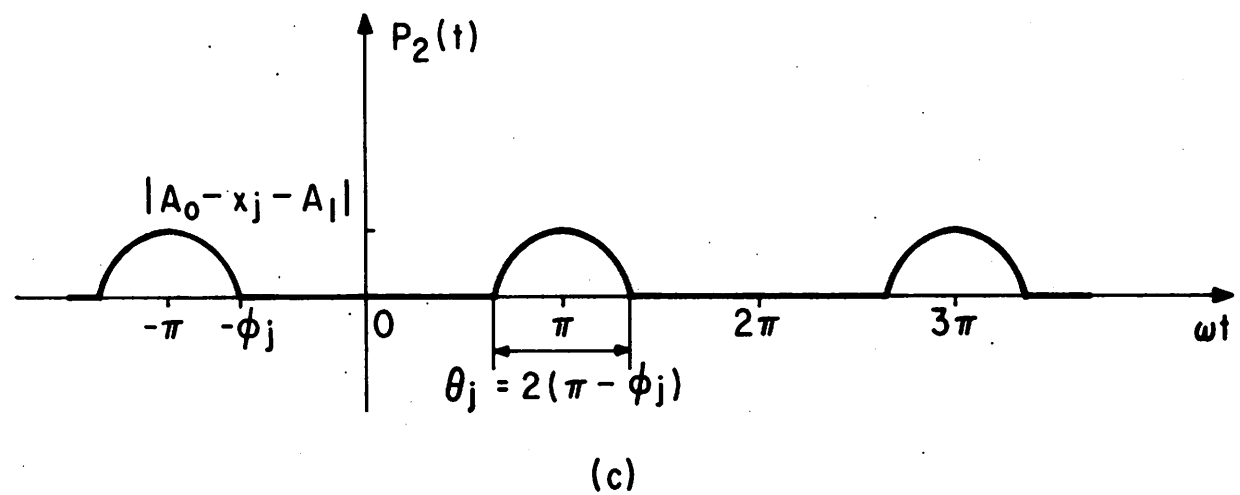
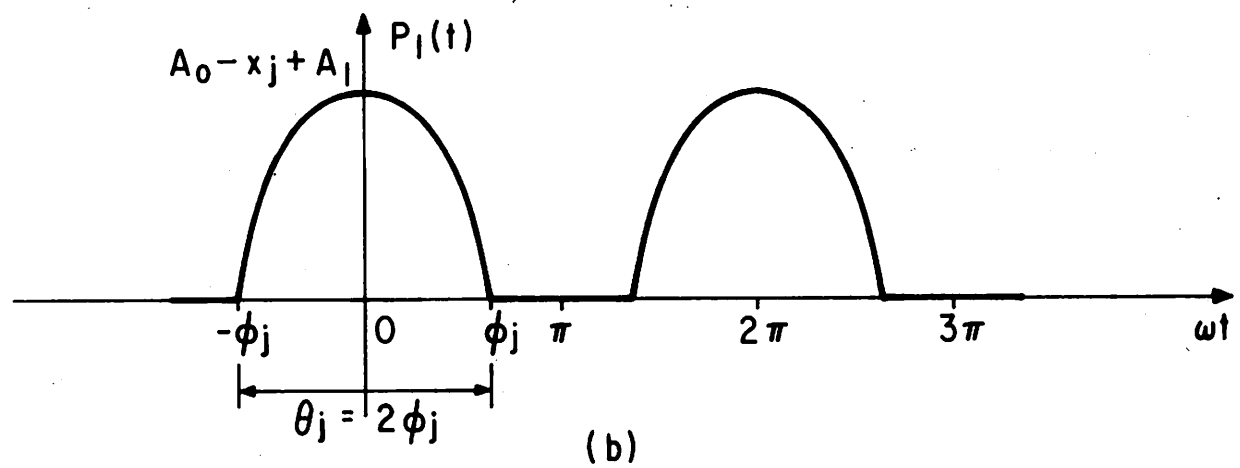
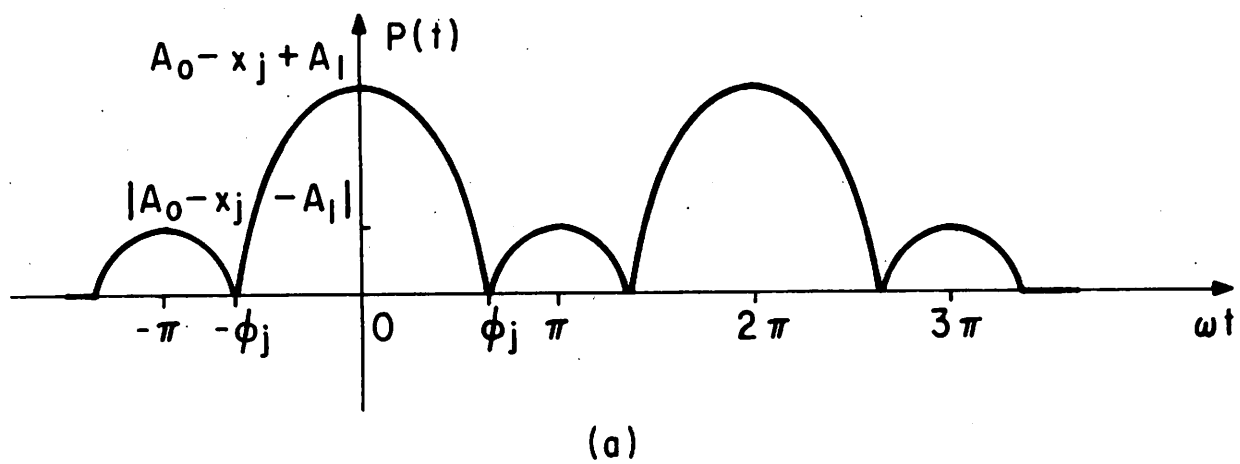


Fig. 8

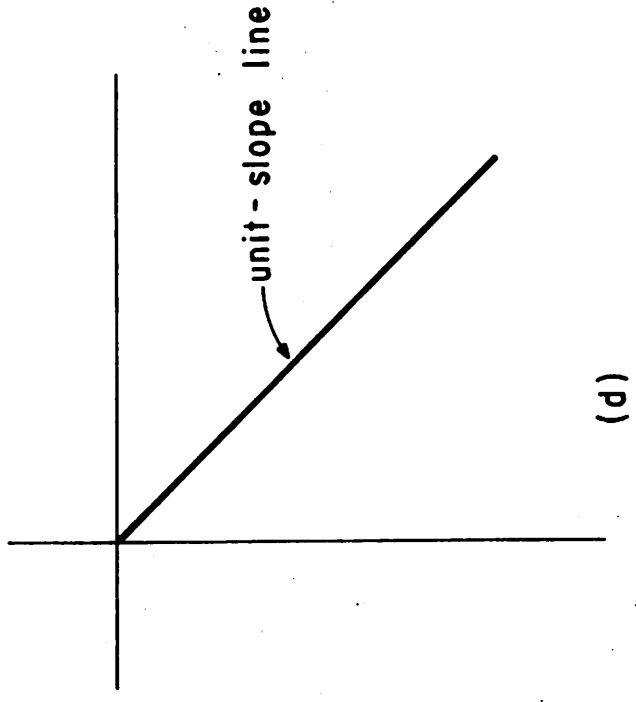
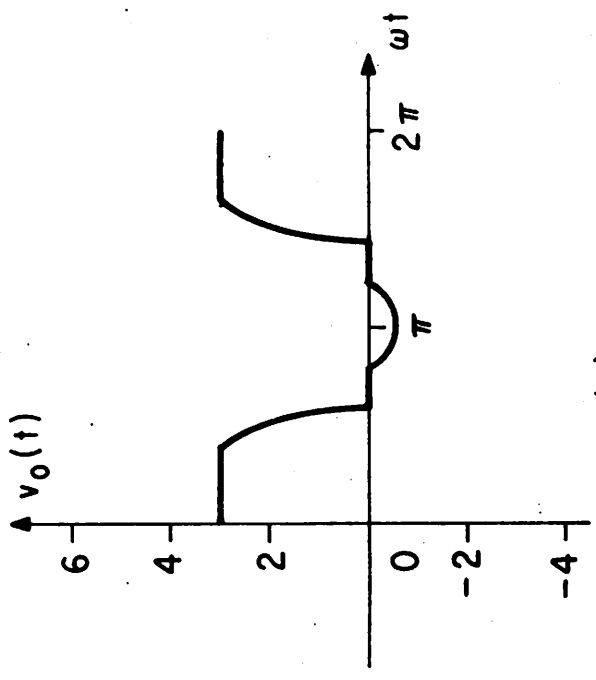
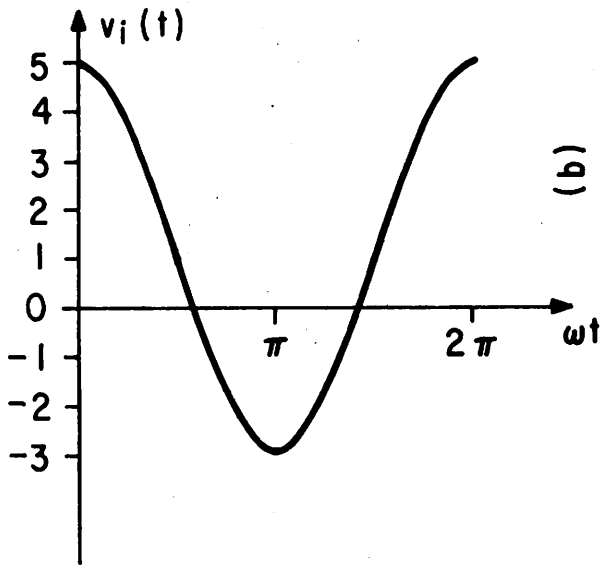
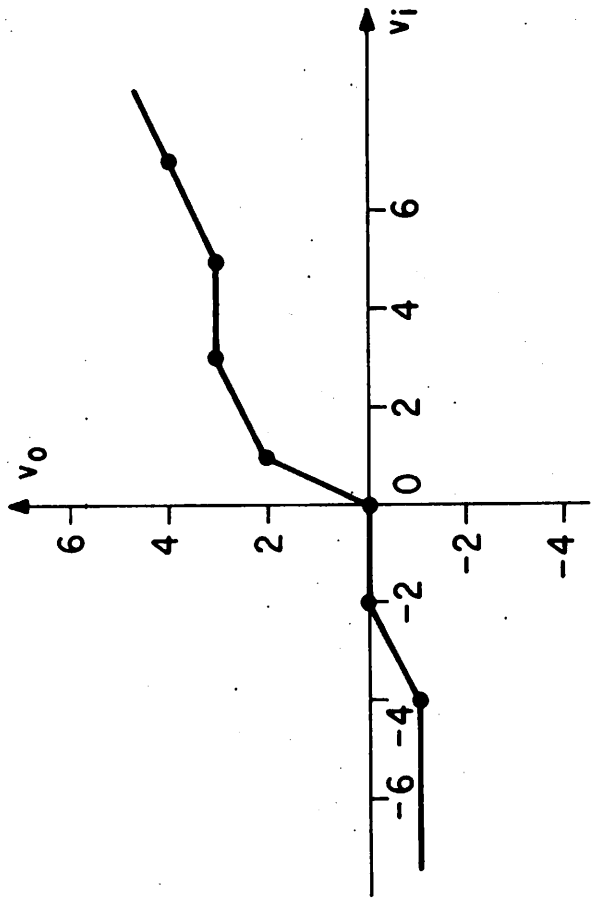
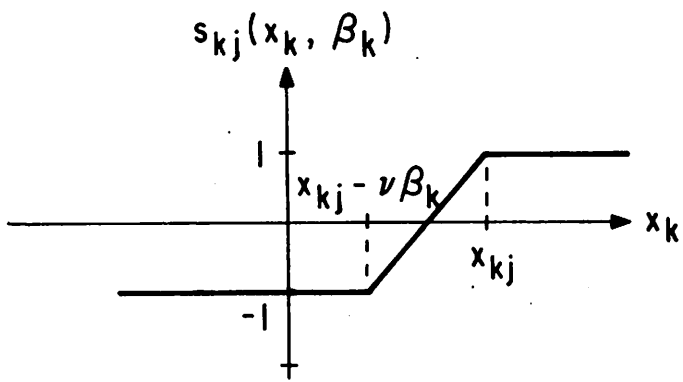
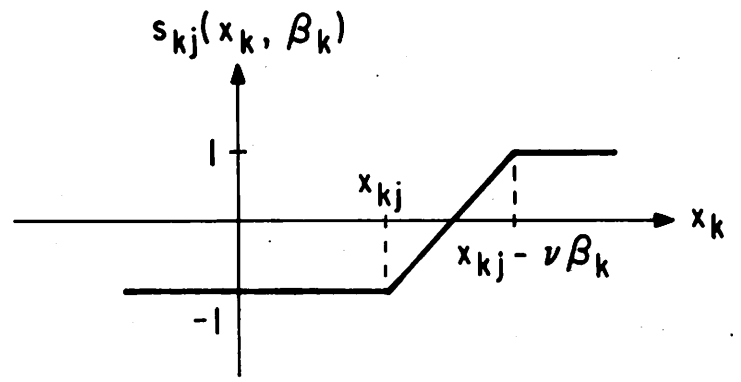


Fig. 9



(a) $\beta_k \geq 0$



(b) $\beta_k < 0$

Fig. A-1